On Covert Rate in Full-Duplex D2D-Enabled Cellular Networks with Spectrum Sharing and Power Control

Ranran Sun, Huihui Wu, Bin Yang, Yulong Shen, Weidong Yang, Xiaohong Jiang, and Tarik Taleb

***Abstract*—This paper investigates the fundamental covert rate performance in a D2D-enabled cellular network consisting of a cellular user Alice, a base station BS, an active warden Willie, and a D2D pair with a transmitter D_t and a full-duplex receiver D_r. To conduct covert communication between Alice and BS, the full-duplex D_r transmits jamming signal to confuse the active Willie and also receives signal from D_t simultaneously. With spectrum sharing, D_t can operate over either an underlay mode reusing cellular spectrum or an overlay mode using dedicated spectrum. With power control, D_r can send jamming signal to confuse Willie's detection of the transmission from Alice. We first provide theoretical results for the outage probabilities of the cellular and D2D transmissions, the average minimum detection error probability at Willie, and the achievable covert rate from Alice to BS. We then explore the power control for covert rate maximization (CRM) under the underlay mode as well as the joint designs of power control and spectrum partition for CRM under the overlay mode. We further consider a mode selection that flexibly switches between these two modes with a probability, and also investigate the covert rate modeling and joint designs of power control, spectrum partition and mode selection probability for CRM. Finally, numerical results are presented to illustrate the covert rate performances of the network under the underlay mode, overlay mode and mode selection.**

This work was supported in part by the National Key Research and Development Program of China under Grant 2023YFB3107500; in part by the National Natural Science Foundation of China under Grant 62220106004, Grant 62372076, Grant 62301402, Grant 62302366, and Grant 62172141; in part by the China Postdoctoral Science Foundation under Grant 2023M742740; in part by the Natural Science Foundation of Henan under Grant 222300420004; in part by the Natural Science Project of Anhui/Chuzhou University under Grant 2020qd16, Grant KJ2021ZD0128, Grant DTR2023051, and Grant 2022XJZD12; This work is partially supported by the European Union's HE research and innovation program HORIZON-JUSNS-2023 under the 6GPath project (Grant No. 101139172). This work was partially conducted at ICTFICIAL Oy. The paper reflects only the authors' views, and the European Commission bears no responsibility for any utilization of the information contained herein. (Corresponding authors: Bin Yang, Yulong Shen.)

R. Sun is with the Hangzhou Institute of Technology, Xidian University, Hangzhou 311231, China (e-mail: srr_2013@163.com).

H. Wu is with Beijing National Research Center for Information Science and Technology (BNRist), Department of Automation, Tsinghua University, Beijing 100084, China (e-mail: hhwu1994@mail.tsinghua.edu.cn).

B. Yang is with the School of Computer and Information Engineering, Chuzhou University, Chuzhou 239000, China (e-mail: yangbinchi@gmail.com).

Y. Shen is with the School of Computer Science and Technology, Xidian University, Xi'an 710071, China (e-mail: ylshen@mail.xidian.edu.cn).

W. Yang is with the Hangzhou Institute of Technology, Xidian University, Hangzhou 311231, China (e-mail: mengguyang@163.com).

X. Jiang is with the School of Systems Information Science, Future University Hakodate, Hakodate 041-8655, Japan (e-mail: jiang@fun.ac.jp).

T. Taleb is with the Faculty of Electrical Engineering and Information Technology, Ruhr University Bochum, Bochum 44801, Germany (e-mail: tarik.taleb@rub.de).

***Index Terms*—Covert communication, full-duplex device-to-device, spectrum sharing, power control.**

I. Introduction

Device-to-device (D2D)-enabled cellular networks have emerged as a promising network architecture to meet the ever increasing demand for mobile data traffic, where proximity users can directly communicate with each other achieving traffic offloading from the base station (BS) [1]–[6]. Such networks have great potentials for improving spectral efficiency, increasing data rate, reducing latency and extending cellular coverage, and thus are highly appealing to serve as the key component of future space-air-ground integrated networks [7], [8]. However, broadcast nature of wireless channels poses a significant security threat to the large amounts of highly sensitive information transmissions from military, finance, self-driving vehicles and healthcare, making the secure information transmissions a paramount important issue in these networks.

The current research works on the secure communications in D2D-enabled cellular networks mainly focus on the protection of wireless transmission content based on the conventional cryptographic approaches [9], [10] or the physical layer security approaches [11]–[14]. The former ones utilize encryption techniques at the upper layers of protocol stack while the latter ones exploit the randomness characteristics of wireless channels to provide protection of data transmissions. Nevertheless, the covert communication that hides the process of wireless transmission itself is also highly desirable for many critical applications, such as secret military operations, covert investigation, and location tracking in vehicular networks. Actually, many kinds of attacks may be launched once the existence of wireless transmission process is exposed to adversaries [15], [16]. Thus, how to achieve covert communication to prevent adversaries from detecting the existence of wireless communications has become increasingly important for D2D-enabled cellular networks [17]. Here, the covert rate and secrecy rate are two important performance metrics for measuring covert communications and secure communications, respectively. The covert rate is defined as the achievable rate under the condition that a transmitter can perform covert communication with its receiver without being detected by the adversary. The secrecy rate is the achievable rate under the condition that the adversary cannot intercept the message from a transmitter to its receiver.

The covert communications have been widely investigated in different wireless networks [18]–[28]. In particular, the work in [20] investigates the covert rate in a two-hop wireless relaying system without the support of the base station (BS), where a source attempts to covertly transmit message to a destination with the help of a relay, and a passive warden detects the covert transmission process. The works of [25]–[28] employ a full-duplex communication technique, where the full-duplex receivers send jamming signal to achieve covert communications. However, only some preliminary works are available on the covert communication studies in D2D-enabled cellular networks [29]–[34]. Under the underlay mode where the D2D users can reuse the spectrum resources of cellular users, the work in [29] proposes a transmit power control scheme for both cellular users and D2D users to maximize the covert rate of D2D transmissions. The work in [30] explores the joint design of spectrum allocation and power control for the maximization of sum covert rate of D2D transmissions, while the work in [31] investigates the user trust degree evaluation and spectrum allocation for such sum covert rate maximization. In [32], the cooperative jamming technique is adopted to send artificial noise to confuse adversaries and to achieve covert rate maximization for D2D transmission. The work in [33] explores the covert rate maximization problem by jointly optimizing the transmit powers of covert signal, jamming signal, and cellular signal in a D2D-enabled cellular system, where a D2D receiver can operate either over the half-duplex mode only receiving message or over the full-duplex mode sending jamming signal to confuse the detection of a warden. Under the overlay mode where the cellular and D2D users can only use their dedicated orthogonal spectrum resources, the work in [34] considers the scenario that the D2D transmitters distributed in a safety area can also serve as relays such that wardens cannot detect the existence of D2D transmissions, and investigates the joint designs of relay selection and transmit power of D2D transmitters to maximize the covert rate of cellular users.

Although these initial works in [29]–[34] are very meaningful in D2D-enabled cellular networks, the covert communications in such networks are still largely unexplored so far. Particularly, underlay and overlay are two fundamental spectrum sharing modes in D2D-enabled cellular networks. The overlay mode adopts orthogonal spectrum allocation for the cellular and D2D links, which reduces the mutual interference between these links and thus improves the data rate performance. The underlay mode adopts spectrum reusing between the cellular and D2D links, which improves the spectrum efficiency but also causes mutual interference between these two links degrading the data rate performance. It is notable that the interference in covert communication can confuse the detection of the warden and thus enhance covertness performance (e.g., detection error probability). The covert rate performance can be further enhanced by designing some schemes, e.g., mode selection between underlay and overlay modes, and power control. Furthermore, in a more practice scenario, warden not only detects covert communication process but also sends noise to interfere with legitimate receiver. As a result, three critical issues arise naturally and need to be carefully explored in the D2D-enabled cellular networks. One issue is how to model the covert rate performance under the underlay and overlay modes in the more practice scenario with an active warden. Another issue is how to optimize the covert rate performance via power control under the two modes. The last issue is how to further enhance the covert performance through a flexible selection of underlay and overlay modes, and power control.

To address these fundamental issues, this paper focuses on the modeling and optimization studies of the covert rate performance under the underlay and overlay modes in the presence of an active warden, where the effects of spectrum partition and sharing, active warden, power control and mode selection are fully taken into account. To protect the covert communication from being detected and attacked by the active warden, the D2D receiver employs the full-duplex communication technique, which simultaneously realizes the transmission of jamming signal and the reception of legitimate signal. Specifically, this paper is different from our previous papers [20], [33]. The paper in [20] focuses on a two-hop wireless relaying system without the support of BS in the presence of a passive warden, while this paper considers a D2D-enabled cellular network with an active warden. The paper in [33] examines the covert D2D communication in a D2D-enabled cellular network with a passive warden and the important issues of spectrum partition and sharing are not carefully considered here. This paper pays attention to the covert cellular communication, and fully considers the two issues that the D2D pair can operate either over the underlay mode or over the overlay mode. The main contributions of this paper are summarized as follows.

- We consider a full-duplex D2D-enabled cellular network consisting of a cellular user, a base station, an active warden Willie, and a D2D pair with a transmitter and a full-duplex (FD) receiver. Here, the FD D2D receiver can simultaneously receive the signal and send jamming signal to confuse Willie's detection of the transmission from Alice. For the concerned network working under either the underlay or overlay mode, we first derive the basic theoretical results for the outage probabilities of the cellular and D2D transmissions, and the average minimum detection error probability at warden.
- Based on above results, we then provide theoretical modeling for the covert rate of cellular link under the underlay mode. The corresponding CRM is formulated as an optimization problem with the constraints of covertness requirement and the transmit power of the FD D2D receiver. We solve the optimization problem based on the rules of differentiation to identify the optimal setting of the transmit power and to derive the analytical result of the maximum covert rate (MCR).
- We further provide theoretical modeling for the covert rate of cellular link under the overlay mode, as well as the related CRM problem with the constraints of covertness requirement, spectrum partition and transmit power of the D2D receiver. By solving the CRM problem, we then determine the optimal settings of the spectrum partition

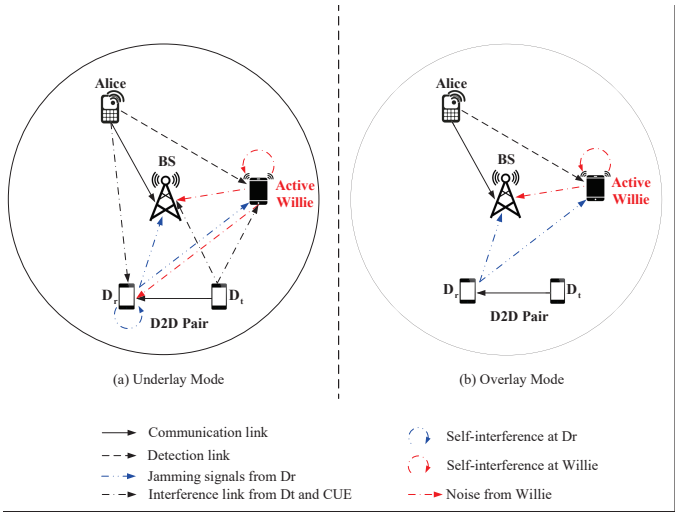

Fig. 1: System model.

and transmit power and thus the analytical expression for MCR.

- For an improvement of covert rate, we consider a flexible mode selection, under which the concerned network can switch between the underlay mode and overlay mode with a certain probability. Under the mode selection, we also explore the related issues of covert rate modeling, CRM formulation and analytical modeling of MCR through jointly optimizing the mode selection probability, spectrum partition and transmit power of the D2D receiver.
- Finally, we present extensive numerical results to illustrate the impacts of spectrum partition, power control and mode selection on the covert rate and the MCR under the underlay mode, overlay mode and mode selection, respectively.

The rest of this paper is organized as follows: Section II introduces the system model. Section III presents some basic results on the detection performance at warden. Section IV and Section V develop theoretical frameworks for covert rate modeling and maximization under the underlay and overlay modes, respectively. We analyze the covert rate and the corresponding MCR under the mode selection in Section VI, and provide numerical results in Section VII. Finally, Section VIII concludes this paper.

II. System Model

A. System Model

As illustrated in Fig. 1, we consider a full-duplex D2D-enabled uplink cellular network consisting of a base station BS, a cellular user Alice, a D2D pair with a transmitter D_t and a full-duplex receiver D_r, and an active warden Willie. Alice seeks to covertly transmit confidential information to BS. Willie, which works in FD mode, receives signal from the network aiming to detect the existence of the transmission from Alice to BS, and emits noise to interfere with BS simultaneously. The D2D pair can conduct information transmission between D_t and D_r, and it can also assist the covert communication of Alice through spectrum sharing with Alice. The full-duplex receiver D_r not only receives information from D_t, but also acts as a friendly jammer to transmit jamming signal to confuse Willie. Both Willie and D_r are equipped with a pair of transmitting and receiving antennas, and each of Alice and D_t has a single antenna.

In our system mode, we consider only one D2D pair instead of the complex scenario where multiple D2D pairs can reuse the resource of a single CU. This is due to the following reasons. The complex scenario poses a great challenge to do the theoretical analysis (e.g., deriving transmission outage probability and optimal detection threshold, solving the optimization problem). However, our work is an initial effort to explore how the mode selection of one D2D pair affects covert rate performance, and can provide many insights for future research. On one hand, we conduct the study of the covert communications in a new D2D network scenario with an active warden. We also explore the covert communications for the first time considering the underlay and overlay modes simultaneously. On the other hand, we theoretically analyze the covert rate performance in the scenario. We also note that previous works [19], [22], [24], [31], [33] mainly focus on simple scenarios, such as the scenario with one transmitter, one receiver and one warden, that with one transmitter, one relay, one receiver and one warden, and that with one D2D pair, one cellular user and one passive warden.

B. Spectrum Sharing

In our study, the cellular user Alice and the D2D transmitter D_t can share the network spectrum in two different modes: underlay and overlay. In underlay mode, D_t reuses the network spectrum occupied by Alice, while for the overlay mode, the network spectrum is partitioned into two orthogonal portions, i.e., a fraction β of the network spectrum is allocated to Alice and the remaining fraction $1-\beta$ is for D_t, where β is a spectrum partition ratio. We further consider a flexible mode selection of spectrum sharing, where D_t can select the underlay mode with probability p and the overlay mode with probability $1-p$. Note that under the mode selection, D_t can find an optimal p such that it can flexibly switch between underlay and overlay modes for maximizing the covert rate from Alice to BS. Willie tries to detect the transmission process of the cellular user. To this end, Willie needs to receive signal from the cellular user Alice and thus uses the same channel as Alice, i.e., they share the same spectrum. This means that under the underlay mode, the D2D pair and Willie use the same channel, and under the overlay mode, they use different channels. Thus, Willie doesn't experience interference from the D2D transmitter D_t under the overlay mode. Moreover, Willie also doesn't experience interference from Alice under the underlay and overlay modes.

Based on the spectrum sharing, there exists mutual interference among different links using the same spectrum. For the underlay mode shown in Fig. 1(a), the total interference experienced by BS is from D_t, D_r and Willie, that experienced by D_r is from Alice, Willie and itself, and that experienced by Willie is from D_t, D_r and itself. As for the overlay mode shown in Fig. 1(b), we consider D_r uses all

available spectrum to transmit jamming signal. Thus, the total interference experienced by BS is from D_r and Willie, and that experienced by Willie is from D_r and itself. Note that in D2D-enabled cellular networks, both the underlay and overlay modes can significantly affect the covert rate performance of the cellular user. Thus, the objective of this paper is to explore how the mode selection of the D2D pair affects the covert rate performance of the cellular network. Specifically, the mode selection will be to maximize the covert rate of the cellular user (CU) while ensuring the Quality-of-Service (QoS) requirement of the D2D pair with no occurring transmission outage. In addition, the underlay and overlay modes are not considered in relay-assisted wireless networks without the support of BS [20]. Thus, the D2D pair cannot be replaced by a simple relay which transmits a jamming signal to Willie.

C. Channel Model

We consider these wireless channels in our concerned network to be quasi-static Rayleigh block fading channels, where each channel coefficient $h_{i,j}$ from a transmitter i to a receiver j remains unchanged in one slot while changing independently from one slot to another. Here, $i \in \{A, D_t, D_r, W\}$ and $j \in \{B, W, D_r\}$, A, B and W denote Alice, BS and Willie, respectively. Under this fading channel model, the channel gain $|h_{i,j}|^2$ is an exponentially distribution random variable with mean $\lambda_{i,j}$ which is known to all nodes, and thus its probability density function (PDF) is given by $f_{|h_{i,j}|^2}(x) = \frac{1}{\lambda_{i,j}} \exp(-\frac{x}{\lambda_{i,j}})$. For simplicity, we use h_{D_r} and h_W to denote the self-interference channel h_{D_r,D_r} and $h_{W,W}$ with the channel gain mean λ_{D_t} and λ_W, respectively. Willie knows instantaneous channel gain $|h_{A,W}|^2$, $|h_{D_r,W}|^2$, $|h_{D_t,W}|^2$, $|h_W|^2$ and statistical CSI of other channels [35]. The instantaneous channel gain known to Willie corresponds to the worst case for Alice. Regarding the rules for power control, mode selection, and spectrum partition fraction, if the covert communication can be achieved under the case that the perfect CSI is known to Willie, it is also achievable under the imperfect channel estimation. Moreover, the covert rate performance can be improved under the imperfect channel estimation. This is because the imperfect channel estimation decreases the detection performance of Willie, such that Alice can use a relatively larger covert transmit power than that under the perfect CSI.

We consider that Alice and D_t employ fixed transmit power P_A and P_{D_t}, respectively. D_r can serve as a jamming node to send artificial noise to confuse Willie to decide whether or not the cellular user Alice covertly transmits message. To this end, the signals that Willie receives should be randomly changing over time. Thus, we treat the transmit power of D_r as a random variable, which obeys a continuous uniform distribution over the interval $[0, P_{\max}^{D_r}]$. Here, $P_{\max}^{D_r}$ will not exceed the inherent maximum transmit power limit Ω of the D2D receiver D_r. This uniform power control model has also been used in previous works [25], [36], [37]. Then, the PDF of P_{D_r} is given by

$$f_P(x) = \begin{cases} \frac{1}{P_{\max}^{D_r}}, & 0 \le x \le P_{\max}^{D_r}, \\ 0, & \text{otherwise.} \end{cases} \tag{1}$$

Willie knows the transmit power distribution of D_r, but cannot be aware of the actual value of P_{D_r} at each slot. To interfere with BS, Willie also employs a variable transmit power P_W, subject to the constraint of maximum value $P_{\max}^W$. In addition, the additive white Gaussian noise at BS, D_r and Willie is denoted by n_B, n_{D_r} and n_W with variance σ_B^2, $\sigma_{D_r}^2$ and σ_W^2, respectively. The total bandwidth of the network spectrum is W MHz. Without loss of generality, we assume $W = 1$ throughout this paper.

D. Detection at Willie

According to the signals received by Willie, it needs to decide whether Alice transmits covert information to BS or not in each slot. Thus, Willie conducts a binary hypothesis testing consisting of a null hypothesis H_0 and an alternative hypothesis H_1. The former H_0 represents that Alice did not transmit covert information to BS, while the latter H_1 represents that Alice did the covert transmission. Consider the underlay and overlay modes, the received signals at Willie under these two hypotheses are expressed as

$$\mathrm{H}_0 : y_W(i) = \begin{cases} \sqrt{P_{D_t}} h_{D_t,W} x_{D_t}(i) + \Delta, & \text{underlay mode,} \\ \Delta, & \text{overlay mode.} \end{cases} \tag{2}$$

$$\mathrm{H}_1 : y_W(i) = \begin{cases} \sqrt{P_A} h_{A,W} x_a(i) \\ \quad + \sqrt{P_{D_t}} h_{D_t,W} x_{D_t}(i) + \Delta, & \text{underlay mode,} \\ \sqrt{P_A} h_{A,W} x_a(i) + \Delta, & \text{overlay mode.} \end{cases} \tag{3}$$

where $\Delta = \sqrt{P_{D_r}} h_{D_r,W} x_{D_r}(i) + \sqrt{\varphi P_{\max}^W} h_W x_W(i) + n_W(i)$. φ is the self-interference cancellation coefficient at Willie, and $\varphi \in [0, 1]$. We consider the worst case that Willie employs a perfect self-interference cancellation technology such that the self-interference at Willie can be completely canceled, i.e., $\varphi = 0$. Due to the negative impact of self-interference at Willie on the detection of covert communication, the complete cancellation of self-interference can achieve a better detection performance at Willie than the partial cancellation. If the covert transmission is successful under the complete cancellation, it can also be successful under the partial cancellation. x_a, x_{D_t}, x_{D_r} and x_W represent the signals transmitted by Alice, D_t, D_r and Willie, respectively. These random variables satisfy that $\mathbb{E}[|x_a(i)|^2] = 1$, $\mathbb{E}[|x_{D_t}(i)|^2] = 1$, $\mathbb{E}[|x_{D_r}(i)|^2] = 1$, and $\mathbb{E}[|x_W(i)|^2] = 1$, where $\mathbb{E}[\cdot]$ denotes an expectation operation. $i = 1, 2, ..., n$ is the index of each received signal at Willie and n is assumed to be infinity, i.e., $n \to \infty$[1]. Since Willie attempts to launch the strongest attack on the legitimate receivers (i.e., BS) as much as possible, the transmit power of Willie corresponds to the maximum value $P_{\max}^W$.

Regarding the observation vector $\mathbf{y_W} = [y_W(1), \ldots, y_W(n)]$, all elements in the vector are independent complex Gaussian random variables with zero mean. The total received power $\sum_{i=1}^n |y_W(i)|^2$ at Willie is a

[1]The assumption can be found in many existing works [19], [20], [25], [29], [32], [33]. $n \to \infty$ indicates that Willie can obtain enough observations from Alice to make the decision, which is the best case for Willie and the worst case for Alice. If Alice can achieve covert communication in $n \to \infty$, the covert communication can also be achieved in the case that n is finite.

sufficient statistic for Willie's test. Since any one-one-function of a sufficient statistic is also a sufficient statistic, the average received power $Y_W = \frac{1}{n}\sum_{i=1}^{n}|y_W(i)|^2$ at Willie is a sufficient statistic. Thus, Willie performs a threshold test on Y_W based on the expression $Y_W \underset{D_0}{\overset{D_1}{\gtrless}} \gamma$, where D_0 and D_1 represent these two decisions of Willie approving H_0 and H_1, respectively, and γ is the detection threshold. We consider an infinite number of received signals at Willie in each slot, i.e., $n \to \infty$, and then the average received power Y_W at Willie under the underlay and overlay modes are given by [38]

$$Y_W = \begin{cases} P_{D_t}|h_{D_t,W}|^2 + P_{D_r}|h_{D_r,W}|^2 + \sigma_W^2, & \mathrm{H}_0, \\ P_A|h_{A,W}|^2 + P_{D_t}|h_{D_t,W}|^2 + P_{D_r}|h_{D_r,W}|^2 + \sigma_W^2, & \mathrm{H}_1, \end{cases} \quad (4)$$

$$\text{and } Y_W = \begin{cases} P_{D_r}|h_{D_r,W}|^2 + \sigma_W^2, & \mathrm{H}_0, \\ P_A|h_{A,W}|^2 + P_{D_r}|h_{D_r,W}|^2 + \sigma_W^2, & \mathrm{H}_1, \end{cases} \quad (5)$$

respectively.

Based on the threshold test and the average received power Y_W, we further define two types of errors: false alarm and missed detection. *False alarm* is defined as the event that Willie makes a decision D_1 to approve H_1 while H_0 is true. The probability of false alarm can be expressed as $\mathbb{P}_{FA} = \mathcal{P}\{Y_W > \gamma|\mathrm{H}_0\}$. *Missed detection* is defined as the event that Willie makes a decision D_0 to approve H_0 while H_1 is true. The probability of missed detection can be expressed as $\mathbb{P}_{MD} = \mathcal{P}\{Y_W < \gamma|\mathrm{H}_1\}$. The sum of $\mathbb{P}_{FA}$ and $\mathbb{P}_{MD}$ (namely detection error probability) are used to measure the detection performance of Willie. Note that the detection error probability depends on the detection threshold γ. Since Alice is hard to know the value of γ, we consider a worst case corresponding to minimum detection error probability at Willie with an optimal γ. Thus, the optimal γ can be determined by minimizing the detection error probability, which is given in Theorem 2. The detailed derivation process can be found in the proof of Theorem 2.

Remark: If multiple D2D pairs are assumed to reuse the spectrum of Alice, the derivation process of the optimal detection threshold γ is given as follows. We also need to consider the worst case corresponding to a minimum detection error probability at Willie which is determined by optimizing the detection threshold γ. Based on the definition of detection error probability, we give the average received power Y_W at Willie as follows.

$$Y_W = \begin{cases} \sum_{m=1}^{M}(P_{D_t}^m|h_{D_t,W}^m|^2 + P_{D_r}^m|h_{D_r,W}^m|^2) + \sigma_W^2, & \mathrm{H}_0, \\ P_A|h_{A,W}|^2 + \sum_{m=1}^{M}(P_{D_t}^m|h_{D_t,W}^m|^2 + P_{D_r}^m|h_{D_r,W}^m|^2) + \sigma_W^2, & \mathrm{H}_1, \end{cases} \quad (6)$$

Then, the probability of false alarm $\mathbb{P}_{FA}$ and the probability of missed detection $\mathbb{P}_{MD}$ can be obtained by utilizing the statistical distribution of the sum of multiple random variables in Y_W. We obtain the expression of the detection error probability equal to the sum of $\mathbb{P}_{FA}$ and $\mathbb{P}_{MD}$. Finally, we identify the optimal detection threshold γ to minimize the detection error probability.

E. Channel Capacity

1) Underlay Mode: Consider the uplink transmission from Alice to BS under the underlay mode, we use SINR_B^u and $\mathrm{SINR}_{D_r}^u$ to denote the instantaneous signal-to-interference-plus-noise-ratio (SINR) at BS and D_r, which are given by

$$\mathrm{SINR}_B^u = \frac{P_A|h_{A,B}|^2}{P_{D_t}|h_{D_t,B}|^2 + P_{D_r}|h_{D_r,B}|^2 + P_{\max}^W|h_{W,B}|^2 + \sigma_B^2}, \quad (7)$$

$$\mathrm{SINR}_{D_r}^u = \frac{P_{D_t}|h_{D_t,D_r}|^2}{P_A|h_{A,D_r}|^2 + \phi P_{D_r}|h_{D_r}|^2 + P_{\max}^W|h_{W,D_r}|^2 + \sigma_{D_r}^2}, \quad (8)$$

where D_r utilizes the self-interference cancellation technology [39] to reduce the negative effect of self-interference. In the technology, ϕ denotes the self-interference cancellation coefficient, and different values of $\phi \in [0,1]$ correspond to different cancellation levels of the self-interference signal. Therefore, the instantaneous channel capacity C_B^u and $C_{D_r}^u$ at BS and D_r are determined as

$$C_B^u = \log_2(1 + \mathrm{SINR}_B^u), \quad (9)$$

and

$$C_{D_r}^u = \log_2(1 + \mathrm{SINR}_{D_r}^u). \quad (10)$$

2) Overlay Mode: As illustrated in Fig. 1(b), under the overlay mode, the SINR at BS and D_r are given by $\mathrm{SINR}_B^o = \frac{P_A|h_{A,B}|^2}{P_{D_r}|h_{D_r,B}|^2 + P_{\max}^W|h_{W,B}|^2 + \sigma_B^2}$ and $\mathrm{SINR}_{D_r}^o = \frac{P_{D_t}|h_{D_t,D_r}|^2}{\sigma_{D_r}^2}$, respectively.

We use C_B^o and $C_{D_r}^o$ to denote the instantaneous channel capacity of the cellular link and that of the D2D link, respectively. We have $C_B^o = \beta\log_2(1 + \mathrm{SINR}_B^o)$ and $C_{D_r}^o = (1-\beta)\log_2(1 + \mathrm{SINR}_{D_r}^o)$.

F. Performance Metrics

We define two performance metrics in terms of detection error probability and covert rate.

Detection error probability: It is the sum of probability of false alarm and that of missed detection, which is expressed as $\mathbb{P}_E = \mathbb{P}_{FA} + \mathbb{P}_{MD}$, where $\mathbb{P}_E$ denotes the detection error probability.

Covert rate: It is the achievable rate from Alice to BS subject to the constraint of covertness requirement which ensures a high detection error probability at Willie.

III. Detection Performance

Under the underlay and overlay modes, we first determine these two probabilities of false alarm and missed detection at Willie. Then, we derive the optimal detection thresholds and corresponding minimum detection error probabilities. Finally, we further derive the average values of the minimum detection error probabilities.

A. Probabilities of False Alarm and Missed Detection

We use $\mathbb{P}_{FA}^u$ and $\mathbb{P}_{MD}^u$ to denote the probability of false alarm and that of missed detection under the underlay mode, respectively. Under the overlay mode, these two probabilities are denoted as $\mathbb{P}_{FA}^o$ and $\mathbb{P}_{MD}^o$, respectively. Then, we determine them in the following Theorem.

Theorem 1. *The probabilities of false alarm and missed detection under the underlay and overlay modes are determined as*

$$\mathbb{P}_{FA}^{u}=\begin{cases}1, & \gamma_u<\alpha_1\\ 1-\frac{\gamma_u-\sigma_W^2-P_{D_t}|h_{D_t,W}|^2}{P_{\max}^{D_r}|h_{D_r,W}|^2}, & \alpha_1\le\gamma_u\le\alpha_3\\ 0, & \gamma_u>\alpha_3\end{cases} \tag{11}$$

$$\mathbb{P}_{MD}^{u}=\begin{cases}0, & \gamma_u<\alpha_2\\ \frac{\gamma_u-\sigma_W^2-P_A|h_{A,W}|^2-P_{D_t}|h_{D_t,W}|^2}{P_{\max}^{D_r}|h_{D_r,W}|^2}, & \alpha_2\le\gamma_u\le\alpha_4\\ 1, & \gamma_u>\alpha_4\end{cases} \tag{12}$$

$$\mathbb{P}_{FA}^{o}=\begin{cases}1, & \gamma_o<\sigma_W^2\\ 1-\frac{\gamma_o-\sigma_W^2}{P_{\max}^{D_r}|h_{D_r,W}|^2}, & \sigma_W^2\le\gamma_o\le\rho_1\\ 0, & \gamma_o>\rho_1\end{cases} \tag{13}$$

$$\mathbb{P}_{MD}^{o}=\begin{cases}0, & \gamma_o<\rho_2\\ \frac{\gamma_o-\sigma_W^2-P_A|h_{A,W}|^2}{P_{\max}^{D_r}|h_{D_r,W}|^2}, & \rho_2\le\gamma_o\le\rho_3\\ 1, & \gamma_o>\rho_3\end{cases} \tag{14}$$

where γ_u and γ_o represent the detection threshold under the underlay and overlay modes, respectively, and

$$\begin{aligned}&\alpha_1=\sigma_W^2+P_{D_t}|h_{D_t,W}|^2,\\ &\alpha_2=\sigma_W^2+P_A|h_{A,W}|^2+P_{D_t}|h_{D_t,W}|^2,\\ &\alpha_3=\sigma_W^2+P_{\max}^{D_r}|h_{D_r,W}|^2+P_{D_t}|h_{D_t,W}|^2,\\ &\alpha_4=\sigma_W^2+P_{\max}^{D_r}|h_{D_r,W}|^2+P_A|h_{A,W}|^2+P_{D_t}|h_{D_t,W}|^2,\\ &\rho_1=P_{\max}^{D_r}|h_{D_r,W}|^2+\sigma_W^2,\quad \rho_2=P_A|h_{A,W}|^2+\sigma_W^2,\\ &\rho_3=P_{\max}^{D_r}|h_{D_r,W}|^2+P_A|h_{A,W}|^2+\sigma_W^2.\end{aligned} \tag{15}$$

Proof. We give the derivation process of these probabilities $\mathbb{P}_{FA}^{u}$ and $\mathbb{P}_{MD}^{u}$ under the underlay mode. According to the definition of the probability of false alarm in Section II-D, we have

$$\begin{aligned}\mathbb{P}_{FA}^{u}&=\mathcal{P}\{Y_W>\gamma_u|\mathrm{H}_0\}\\ &=\mathcal{P}\{P_{D_t}|h_{D_t,W}|^2+P_{D_r}|h_{D_r,W}|^2+\sigma_W^2>\gamma_u\}\\ &=\mathcal{P}\{P_{D_r}>\omega\}=\begin{cases}1, & \gamma_u<\alpha_1\\ \int_{\omega}^{P_{\max}^{D_r}}f_P(x)\mathrm{d}x, & \alpha_1\le\gamma_u\le\alpha_3\\ 0, & \text{otherwise}\end{cases}\end{aligned} \tag{16}$$

where $\omega=\frac{\gamma_u-\sigma_W^2-P_{D_t}|h_{D_t,W}|^2}{|h_{D_r,W}|^2}$.

We further determine the probability of missed detection as

$$\begin{aligned}&\mathbb{P}_{MD}^{u}=\mathcal{P}\{Y_W<\gamma_u|\mathrm{H}_1\}\\ &=\mathcal{P}\{P_A|h_{A,W}|^2+P_{D_t}|h_{D_t,W}|^2+P_{D_r}|h_{D_r,W}|^2+\sigma_W^2<\gamma_u\}\\ &=\mathcal{P}\{P_{D_r}<\Lambda\}=\begin{cases}0, & \gamma_u<\alpha_2\\ \int_0^{\Lambda}f_P(x)\mathrm{d}x, & \alpha_2\le\gamma_u\le\alpha_4\\ 1, & \text{otherwise}\end{cases}\end{aligned} \tag{17}$$

where $\Lambda=\frac{\gamma_u-\sigma_W^2-P_A|h_{A,W}|^2-P_{D_t}|h_{D_t,W}|^2}{|h_{D_r,W}|^2}$, and $f_P(x)$ is the PDF of jamming signal at D_r defined in (1). Thus, we can obtain $\mathbb{P}_{FA}^{u}$ and $\mathbb{P}_{MD}^{u}$.

The derivation process of these probabilities $\mathbb{P}_{FA}^{o}$ and $\mathbb{P}_{MD}^{o}$ is similar to that of $\mathbb{P}_{FA}^{u}$ and $\mathbb{P}_{MD}^{u}$. Thus, we omit it here. □

B. Optimal Detection Thresholds and Minimum Detection Error Probabilities

We use γ_u^* and γ_o^* to denote the optimal detection threshold at Willie under the underlay and overlay modes, respectively. The optimal detection thresholds and corresponding minimum detection error probabilities are given in the following Theorem.

Theorem 2. *The optimal detection thresholds at Willie under the underlay and overlay modes are determined as*

$$\gamma_u^*\in\begin{cases}[\alpha_2,\alpha_3], & \alpha_3>\alpha_2\\ [\alpha_3,\alpha_2], & \alpha_2>\alpha_3\end{cases} \tag{18}$$

$$\gamma_o^*\in\begin{cases}[\rho_2,\rho_1], & \rho_1>\rho_2\\ [\rho_1,\rho_2], & \rho_2>\rho_1\end{cases} \tag{19}$$

where the variables α_2, α_3, ρ_1 and ρ_2 are defined in (15). Specifically, when $\alpha_3>\alpha_2$ or $\rho_1>\rho_2$, we have $P_{\max}^{D_r}>\frac{P_A|h_{A,W}|^2}{|h_{D_r,W}|^2}$. Given these optimal thresholds, both the minimum detection error probabilities $\mathbb{P}_E^*$ under the underlay and overlay modes have the same expression, which is given by

$$\mathbb{P}_E^*=\begin{cases}1-\frac{P_A|h_{A,W}|^2}{P_{\max}^{D_r}|h_{D_r,W}|^2}, & \alpha_3>\alpha_2 \text{ or } \rho_1>\rho_2\\ 0, & \alpha_2>\alpha_3 \text{ or } \rho_2>\rho_1\end{cases} \tag{20}$$

Proof. We first derive the optimal detection threshold γ_u^* and the minimum detection error probability $\mathbb{P}_E^*$ under the underlay mode. Based on the definition of detection error probability and the main results of $\mathbb{P}_{FA}^{u}$ and $\mathbb{P}_{MD}^{u}$ in Theorem 1, we can obtain the detection error probability $\mathbb{P}_E^u$ in the following two cases: $\alpha_3>\alpha_2$ and $\alpha_2>\alpha_3$.

When $\alpha_3>\alpha_2$, $\mathbb{P}_E^u$ can be determined as

$$\mathbb{P}_E^u=\begin{cases}1, & \gamma_u\le\alpha_1\\ 1-\frac{\gamma_u-\sigma_W^2-P_{D_t}|h_{D_t,W}|^2}{P_{\max}^{D_r}|h_{D_r,W}|^2}, & \alpha_1<\gamma_u\le\alpha_2\\ 1-\frac{P_A|h_{A,W}|^2}{P_{\max}^{D_r}|h_{D_r,W}|^2}, & \alpha_2<\gamma_u<\alpha_3\\ \frac{\gamma_u-\sigma_W^2-P_A|h_{A,W}|^2-P_{D_t}|h_{D_t,W}|^2}{P_{\max}^{D_r}|h_{D_r,W}|^2}, & \alpha_3\le\gamma_u<\alpha_4\\ 1. & \gamma_u\ge\alpha_4\end{cases} \tag{21}$$

Following (21), we have $\frac{\partial\mathbb{P}_E^u}{\partial\gamma_u}<0$, when $\gamma_u\in(\alpha_1,\alpha_2]$. This means that $\mathbb{P}_E^u$ decreases as γ_u increases. When $\gamma_u\in[\alpha_3,\alpha_4)$, $\frac{\partial\mathbb{P}_E^u}{\partial\gamma_u}>0$, indicating that $\mathbb{P}_E^u$ increases as γ_u increases. Thus, we obtain the minimum detection error probability $\mathbb{P}_E^*=1-\frac{P_A|h_{A,W}|^2}{P_{\max}^{D_r}|h_{D_r,W}|^2}$, where the optimal detection threshold $\gamma_u^*\in[\alpha_2,\alpha_3]$. Based on $\alpha_3>\alpha_2$ and the expressions of α_2 and α_3 defined in (15), we have $P_{\max}^{D_r}>\frac{P_A|h_{A,W}|^2}{|h_{D_r,W}|^2}$.

When $\alpha_2>\alpha_3$, $\mathbb{P}_E^u$ can be determined as

$$\mathbb{P}_E^u=\begin{cases}1, & \gamma_u\le\alpha_1\\ 1-\frac{\gamma_u-\sigma_W^2-P_{D_t}|h_{D_t,W}|^2}{P_{\max}^{D_r}|h_{D_r,W}|^2}, & \alpha_1<\gamma_u\le\alpha_3\\ 0, & \alpha_3<\gamma_u<\alpha_2\\ \frac{\gamma_u-\sigma_W^2-P_A|h_{A,W}|^2-P_{D_t}|h_{D_t,W}|^2}{P_{\max}^{D_r}|h_{D_r,W}|^2}, & \alpha_2\le\gamma_u<\alpha_4\\ 1, & \gamma_u\ge\alpha_4\end{cases} \tag{22}$$

Based on (22), we can also obtain the minimum detection error probability $\mathbb{P}_E^* = 0$ where the optimal detection threshold $\gamma_u^* \in [\alpha_3, \alpha_2]$.

Since the derivation process of the optimal threshold γ_o^* and the minimum detection error probability $\mathbb{P}_E^*$ under the overlay mode are similar to that under the underlay mode, thus we omit it here. □

An interesting finding from Theorem 2 indicates that the minimum detection error probabilities at Willie under the underlay and overlay modes have the same value. This is due to the following reasons. As shown in Fig. 1, we can see that under the underlay mode, the received signals at Willie are from Alice, itself, D_t and D_r, while under the overlay mode, they are from Alice, itself and D_r. However, since D_t employs a fixed transmit power and $n \to \infty$, Willie could observe the signal statistic from D_t over long periods of time. Thus, the signal from D_t does not affect the detection error probability at Willie, which leads to an identical minimum detection error probability under the underlay and overlay modes.

C. Average Minimum Detection Error Probability

The average minimum detection error probability $\overline{\mathbb{P}}_E^*$ is equivalent to the expected value of the minimum detection error probability $\mathbb{P}_E^*$ under the underlay and overlay modes, which is derived in the following Theorem.

Theorem 3. *The average minimum detection error probability $\overline{\mathbb{P}}_E^*$ at Willie is determined as*

$$\overline{\mathbb{P}}_E^* = \frac{P_{\max}^{D_r}\lambda_{D_r,W}}{P_{\max}^{D_r}\lambda_{D_r,W} + P_A\lambda_{A,W}} + \frac{P_{\max}^{D_r}\lambda_{D_r,W}P_A\lambda_{A,W}}{(P_{\max}^{D_r}\lambda_{D_r,W} + P_A\lambda_{A,W})^2} + \frac{P_A\lambda_{A,W}}{P_{\max}^{D_r}\lambda_{D_r,W} + P_A\lambda_{A,W}} \ln \frac{P_A\lambda_{A,W}}{P_{\max}^{D_r}\lambda_{D_r,W} + P_A\lambda_{A,W}} \tag{23}$$

Proof. $\mathbb{P}_E^*$ given in (20) is a function of random variables $|h_{A,W}|^2$ and $|h_{D_r,W}|^2$. The average minimum detection error probability $\overline{\mathbb{P}}_E^*$ is the expected value $\mathbb{E}[\mathbb{P}_E^*]$ of $\mathbb{P}_E^*$, i.e.,

$$\begin{aligned}\overline{\mathbb{P}}_E^* &= \mathcal{P}\left\{P_{\max}^{D_r} > \frac{P_A|h_{A,W}|^2}{|h_{D_r,W}|^2}\right\} \times \mathbb{E}\left[1 - \frac{P_A|h_{A,W}|^2}{P_{\max}^{D_r}|h_{D_r,W}|^2}\middle| P_{\max}^{D_r} > \frac{P_A|h_{A,W}|^2}{|h_{D_r,W}|^2}\right] \\ &\quad + \mathcal{P}\left\{P_{\max}^{D_r} \le \frac{P_A|h_{A,W}|^2}{|h_{D_r,W}|^2}\right\}\mathbb{E}\left[0\middle| P_{\max}^{D_r} \le \frac{P_A|h_{A,W}|^2}{|h_{D_r,W}|^2}\right] \\ &= \mathcal{P}\left\{P_{\max}^{D_r} > \frac{P_A|h_{A,W}|^2}{|h_{D_r,W}|^2}\right\} \times \mathbb{E}\left[1 - \frac{P_A|h_{A,W}|^2}{P_{\max}^{D_r}|h_{D_r,W}|^2}\middle| P_{\max}^{D_r} > \frac{P_A|h_{A,W}|^2}{|h_{D_r,W}|^2}\right].\end{aligned} \tag{24}$$

Since

$$\begin{aligned}&\mathcal{P}\left\{P_{\max}^{D_r} > \frac{P_A|h_{A,W}|^2}{|h_{D_r,W}|^2}\right\} \\ &= \mathcal{P}\left\{|h_{A,W}|^2 < \frac{P_{\max}^{D_r}|h_{D_r,W}|^2}{P_A}\right\} \\ &= \int_0^\infty \int_0^{\frac{P_{\max}^{D_r}}{P_A}y} f_{|h_{A,W}|^2}(x) f_{|h_{D_r,W}|^2}(y)\mathrm{d}x\mathrm{d}y \\ &= 1 - \frac{P_A\lambda_{A,W}}{P_{\max}^{D_r}\lambda_{D_r,W} + P_A\lambda_{A,W}},\end{aligned} \tag{25}$$

and

$$\begin{aligned}&\mathbb{E}\left[1 - \frac{P_A|h_{A,W}|^2}{P_{\max}^{D_r}|h_{D_r,W}|^2}\middle| P_{\max}^{D_r} > \frac{P_A|h_{A,W}|^2}{|h_{D_r,W}|^2}\right] \\ &= 1 - \mathbb{E}\left[\frac{P_A|h_{A,W}|^2}{P_{\max}^{D_r}|h_{D_r,W}|^2}\middle| P_{\max}^{D_r} > \frac{P_A|h_{A,W}|^2}{|h_{D_r,W}|^2}\right] \\ &= 1 - \frac{P_A}{P_{\max}^{D_r}}\int_0^\infty \int_0^{\frac{P_{\max}^{D_r}}{P_A}y} \frac{x}{y} f_{|h_{A,W}|^2}(x) f_{|h_{D_r,W}|^2}(y)\mathrm{d}x\mathrm{d}y \\ &= 1 - \frac{P_A\lambda_{A,W}}{P_{\max}^{D_r}\lambda_{D_r,W}}\left[\ln\left(1 + \frac{P_{\max}^{D_r}\lambda_{D_r,W}}{P_A\lambda_{A,W}}\right) - \frac{P_{\max}^{D_r}\lambda_{D_r,W}}{P_{\max}^{D_r}\lambda_{D_r,W} + P_A\lambda_{A,W}}\right].\end{aligned} \tag{26}$$

By substituting (25) and (26) into (24), (23) follows. □

To achieve covert transmission, the covertness requirement should be satisfied, i.e., for any $\varepsilon \ge 0$, $\overline{\mathbb{P}}_E^* \ge 1 - \varepsilon$, as $n \to \infty$ [40].

IV. Covert Rate under the Underlay Mode

In this section, we first provide theoretical modeling for the covert rate of cellular link from Alice to BS under the underlay mode, and then optimize transmit power of D_r for maximizing the covert rate.

A. Covert Rate Modeling

We use R_C^u to denote the covert rate of the cellular link under the underlay mode. To ensure the quality of D2D link, we define R_C^u is the product of the desirable covert rate, no outage probability of the cellular link and no outage probability of the D2D link [32]. Then, R_C^u can be formulated as

$$R_C^u = R_B(1 - P_{co}^u)(1 - P_{do}^u), \tag{27}$$

where R_B is the desirable rate from Alice to BS, P_{co}^u is the transmission outage probability of the cellular link and P_{do}^u is that of the D2D link.

To derive the covert rate R_C^u, we need to determine the transmission outage probabilities of P_{co}^u and P_{do}^u. The transmission outage probability P_{ou} of a link is defined as the probability that the instantaneous channel capacity C of the link is less than its desirable rate R, i.e.,

$$P_{ou} = \mathcal{P}\{C < R\}. \tag{28}$$

Then, we can obtain P_{co}^u and P_{do}^u in the following Theorem 4.

Theorem 4. *Under the underlay mode, the transmission outage probability P_{co}^{u} of the cellular link and P_{do}^{u} of the D2D link are given by*

$$P_{co}^{u}=1-\frac{\lambda_{A,B}^{3}\exp(-\frac{\mu\sigma_{B}^{2}}{\lambda_{A,B}})\ln(1+\frac{\mu P_{\max}^{D_r}\lambda_{D_r,B}}{\lambda_{A,B}})}{\mu P_{\max}^{D_r}\lambda_{D_r,B}(\mu P_{D_t}\lambda_{D_t,B}+\lambda_{A,B})(\mu P_{\max}^{W}\lambda_{W,B}+\lambda_{A,B})}, \tag{29}$$

$$P_{do}^{u}=1-\frac{\lambda_{D_t,D_r}^{3}\exp(-\frac{\kappa\sigma_{D_r}^{2}}{\lambda_{D_t,D_r}})\ln(1+\frac{\kappa\phi P_{\max}^{D_r}\lambda_{D_r}}{\lambda_{D_t,D_r}})}{(\kappa P_{A}\lambda_{A,D_r}+\lambda_{D_t,D_r})(\kappa P_{\max}^{D_r}\lambda_{W,D_r}+\lambda_{D_t,D_r})\kappa\phi P_{\max}^{D_r}\lambda_{D_r}}, \tag{30}$$

where $\mu=\frac{2^{R_B}-1}{P_A}$, $\kappa=\frac{2^{R_D}-1}{P_{D_t}}$, R_D is the desirable rate of the D2D link and ϕ is the self-interference cancellation coefficient.

Proof. According to the definition of transmission outage probability in (28), the transmission outage probability P_{co}^{u} and P_{do}^{u} are formulated as $P_{co}^{u}=\mathcal{P}\{C_B^u<R_B\}$ and $P_{do}^{u}=\mathcal{P}\{C_{D_r}^u<R_D\}$, respectively. Where C_B^u and $C_{D_r}^u$ are the instantaneous channel capacity of the cellular link and the D2D link under the underlay mode, which are given in (9) and (10). Thus we have

$$\begin{aligned}
&P_{co}^{u}=\mathcal{P}\{\log_2(1+\mathrm{SINR}_B^u)<R_B\}\\
&=\mathcal{P}\{\mathrm{SINR}_B^u<2^{R_B}-1\}\\
&=\mathcal{P}\{|h_{A,B}|^2<\mu(P_{D_t}|h_{D_t,B}|^2+P_{D_r}|h_{D_r,B}|^2+P_{\max}^{W}|h_{W,B}|^2+\sigma_B^2)\}\\
&=\int_0^{P_{\max}^{D_r}}\int_0^{\infty}\int_0^{\infty}\int_0^{\infty}\int_0^{\Theta}f_{|h_{A,B}|^2}(x)f_{|h_{D_t,B}|^2}(y)\\
&\times f_{|h_{D_r,B}|^2}(z)f_{|h_{W,B}|^2}(w)f_P(P_{D_r})\mathrm{d}x\mathrm{d}y\mathrm{d}z\mathrm{d}w\mathrm{d}P_{D_r},
\end{aligned} \tag{31}$$

and

$$\begin{aligned}
&P_{do}^{u}=\mathcal{P}\{\log_2(1+\mathrm{SINR}_{D_r}^u)<R_D\}\\
&=\mathcal{P}\{\mathrm{SINR}_{D_r}^u<2^{R_D}-1\}\\
&=\mathcal{P}\{|h_{D_t,D_r}|^2<\Psi\}\\
&=\int_0^{P_{\max}^{D_r}}\int_0^{\infty}\int_0^{\infty}\int_0^{\infty}\int_0^{\Psi}f_{|h_{D_t,D_r}|^2}(x)f_{|h_{A,D_r}|^2}(y)\\
&\times f_{|h_{D_r}|^2}(z)f_{|h_{W,D_r}|^2}(w)f_P(P_{D_r})\mathrm{d}x\mathrm{d}y\mathrm{d}z\mathrm{d}w\mathrm{d}P_{D_r},
\end{aligned} \tag{32}$$

where $\Theta=\mu(P_{D_t}y+P_{D_r}z+P_{\max}^{W}w+\sigma_B^2)$, $\Psi=\kappa(P_A|h_{A,D_r}|^2+\phi P_{D_r}|h_{D_r}|^2+P_{\max}^{W}|h_{W,D_r}|^2+\sigma_{D_r}^2)$. By solving (31) and (32), (29) and (30) follow. □

B. Covert Rate Maximization

Our objective is to maximize the covert rate of the cellular link by optimizing the maximum transmit power of D_r, where an optimal maximum transmit power ensures that the jamming signal emitted by D_r can confuse the detection of Willie and reduce its interference to the cellular and D2D communications as much as possible. Thus, the CRM can be formulated as the following nonlinear optimization problem

$$\max_{P_{\max}^{D_r}} \quad R_C^u, \tag{33a}$$

$$\text{s.t.} \quad \overline{\mathbb{P}}_E^{*}\geq 1-\varepsilon, \tag{33b}$$

$$0\leq P_{\max}^{D_r}\leq\Omega, \tag{33c}$$

where R_C^u is the covert rate of the cellular link given in (27), and Ω denotes the upper bound of $P_{\max}^{D_r}$. Constraint (33b) ensures that the average minimum detection error probability $\overline{\mathbb{P}}_E^{*}$ is no less than a predetermined value, where ε is an arbitrarily small covertness requirement. Constraint (33c) gives the range of $P_{\max}^{D_r}$.

The solution of the optimization problem is given in the following Theorem.

Theorem 5. *We use $P_{\max}^{D_r u*}$ to denote the optimal maximum transmit power of D_r under the underlay mode.*

When $f(\varepsilon)\leq\Omega$,

$$P_{\max}^{D_r u*}=f(\varepsilon), \tag{34}$$

where $f(\varepsilon)$ is the solution of $\overline{\mathbb{P}}_E^{*}=1-\varepsilon$. The corresponding MCR R_C^{u*} is obtained by substituting $P_{\max}^{D_r u*}$ into (27).

When $f(\varepsilon)>\Omega$, any $P_{\max}^{D_r u*}\in[0,\Omega]$ cannot satisfy the covertness requirement of (33b), and thus $R_C^{u*}=0$.

Proof. To maximize the objective function in (33a), we first decide whether R_C^u is a monotonous function with respect to $P_{\max}^{D_r}$. Thus, we have

$$\frac{\partial R_C^u}{\partial P_{\max}^{D_r}}=R_B[-\frac{\partial P_{co}^{u}}{\partial P_{\max}^{D_r}}(1-P_{do}^{u})+(1-P_{co}^{u})(-\frac{\partial P_{do}^{u}}{\partial P_{\max}^{D_r}})]. \tag{35}$$

We know that $R_B>0$, $0\leq P_{co}^{u}\leq 1$ and $0\leq P_{do}^{u}\leq 1$. Now we only need to determine the signs of $\frac{\partial P_{co}^{u}}{\partial P_{\max}^{D_r}}$ and $\frac{\partial P_{do}^{u}}{\partial P_{\max}^{D_r}}$. To this end, we have

$$\frac{\partial P_{co}^{u}}{\partial P_{\max}^{D_r}}=-t_1(\frac{\mu P_{\max}^{D_r}\lambda_{D_r,B}}{\lambda_{A,B}+\mu P_{\max}^{D_r}\lambda_{D_r,B}}-\ln(1+\frac{\mu P_{\max}^{D_r}\lambda_{D_r,B}}{\lambda_{A,B}})) \tag{36}$$

where $t_1=\frac{\lambda_{A,B}^{3}\exp(-\frac{\mu\sigma_B^2}{\lambda_{A,B}})\mu\lambda_{D_r,B}(\mu P_{D_t}\lambda_{D_t,B}+\lambda_{A,B})(\mu P_{\max}^{W}\lambda_{W,B}+\lambda_{A,B})}{(\mu P_{\max}^{D_r}\lambda_{D_r,B}(\mu P_{D_t}\lambda_{D_t,B}+\lambda_{A,B})(\mu P_{\max}^{W}\lambda_{W,B}+\lambda_{A,B}))^2}>0$. According to the inequality $\ln(1+x)>\frac{x}{1+x}$, we have $\frac{\mu P_{\max}^{D_r}\lambda_{D_r,B}}{\lambda_{A,B}+\mu P_{\max}^{D_r}\lambda_{D_r,B}}-\ln(1+\frac{\mu P_{\max}^{D_r}\lambda_{D_r,B}}{\lambda_{A,B}})<0$. Thus, $\frac{\partial P_{co}^{u}}{\partial P_{\max}^{D_r}}>0$.

We continue to determine $\frac{\partial P_{do}^{u}}{\partial P_{\max}^{D_r}}$ as

$$\frac{\partial P_{do}^{u}}{\partial P_{\max}^{D_r}}=-t_2(\frac{\kappa\phi P_{\max}^{D_r}\lambda_{D_r}}{\lambda_{D_t,D_r}+\kappa\phi P_{\max}^{D_r}\lambda_{D_r}}-\ln(1+\frac{\kappa\phi P_{\max}^{D_r}\lambda_{D_r}}{\lambda_{D_t,D_r}})), \tag{37}$$

where $t_2=\frac{\lambda_{D_t,D_r}^{3}\kappa\phi\lambda_{D_r}\zeta_1\zeta_2\exp(-\frac{\kappa\sigma_{D_r}^2}{\lambda_{D_t,D_r}})}{(\zeta_1\zeta_2\kappa\phi P_{\max}^{D_r}\lambda_{D_r})^2}>0$, $\zeta_1=\kappa P_A\lambda_{A,D_r}+\lambda_{D_t,D_r}$, $\zeta_2=\kappa P_{\max}^{W}\lambda_{W,D_r}+\lambda_{D_t,D_r}$. Applying the inequality $\ln(1+x)>\frac{x}{1+x}$, we obtain $\frac{\kappa\phi P_{\max}^{D_r}\lambda_{D_r}}{\lambda_{D_t,D_r}+\kappa\phi P_{\max}^{D_r}\lambda_{D_r}}-\ln(1+\frac{\kappa\phi P_{\max}^{D_r}\lambda_{D_r}}{\lambda_{D_t,D_r}})<0$. Therefore, $\frac{\partial P_{do}^{u}}{\partial P_{\max}^{D_r}}>0$.

Since both the signs of $\frac{\partial P_{co}^{u}}{\partial P_{\max}^{D_r}}$ and $\frac{\partial P_{do}^{u}}{\partial P_{\max}^{D_r}}$ are positive, $\frac{\partial R_C^u}{\partial P_{\max}^{D_r}}<0$. Thus, R_C^u is a monotonically decreasing function of $P_{\max}^{D_r}$.

Next, we decide whether $\overline{\mathbb{P}}_E^{*}$ is a monotonous function with respect to $P_{\max}^{D_r}$. Thus, we have

$$\begin{aligned}
\frac{\partial\overline{\mathbb{P}}_E^{*}}{\partial P_{\max}^{D_r}}=&\frac{P_A\lambda_{A,W}\lambda_{D_r,W}}{(P_{\max}^{D_r}\lambda_{D_r,W}+P_A\lambda_{A,W})^2}\Big[\frac{P_A\lambda_{A,W}-P_{\max}^{D_r}\lambda_{D_r,W}}{P_{\max}^{D_r}\lambda_{D_r,W}+P_A\lambda_{A,W}}\\
&+\ln(1+\frac{P_{\max}^{D_r}\lambda_{D_r,W}}{P_A\lambda_{A,W}})\Big]
\end{aligned} \tag{38}$$

Applying the inequality $\ln(1+x) > \frac{x}{1+x}$, we obtain $\frac{\partial \overline{\mathbb{P}}_E^*}{\partial P_{\max}^{D_r}} > 0$, which reveals that $\overline{\mathbb{P}}_E^*$ is a monotonically increasing function of $P_{\max}^{D_r}$. Thus, the feasible solution of (33b) satisfies $P_{\max}^{D_r} \geq f(\varepsilon)$. Note that R_C^u monotonically decreases with $P_{\max}^{D_r}$ and the upper bound of $P_{\max}^{D_r}$ is Ω. When $f(\varepsilon) \leq \Omega$, the optimal maximum transmit power of D_r is determined as $P_{\max}^{D_r u*} = f(\varepsilon)$. The corresponding MCR R_C^{u*} follows by substituting $P_{\max}^{D_r u*}$ into (27). When $f(\varepsilon) > \Omega$, any $P_{\max}^{D_r u*} \in [0, \Omega]$ cannot satisfy the covertness requirement of (33b), and thus $R_C^{u*} = 0$. □

V. Covert Rate under the Overlay Mode

In this section, we first provide theoretical modeling for the covert rate of cellular link from Alice to BS under the overlay mode, and then optimize the spectrum partition and transmit power of D_r for maximizing the covert rate.

A. Covert Rate Modeling

We use R_C^o to denote the covert rate of the cellular link from Alice to Bob under the overlay mode, and then we formulate the covert rate as

$$R_C^o = R_B(1 - P_{co}^o)(1 - P_{do}^o), \tag{39}$$

where P_{co}^o and P_{do}^o are the transmission outage probabilities of the cellular link and the D2D link under the overlay mode, respectively.

To derive the covert rate R_C^o, we need to determine P_{co}^o and P_{do}^o in the following theorem.

Theorem 6. *The transmission outage probability P_{co}^o of the cellular link and P_{do}^o of the D2D link under the overlay mode are given by*

$$P_{co}^o = 1 - \frac{\lambda_{A,B}^2 \exp(-\frac{\theta\sigma_B^2}{\lambda_{A,B}}) \ln(1 + \frac{\theta P_{\max}^{D_r} \lambda_{D_r,B}}{\lambda_{A,B}})}{\theta P_{\max}^{D_r} \lambda_{D_r,B}(\theta P_{\max}^{W} \lambda_{W,B} + \lambda_{A,B})} \tag{40}$$

$$P_{do}^o = 1 - \exp(-\frac{\eta\sigma_{D_r}^2}{\lambda_{D_t,D_r}}) \tag{41}$$

where $\theta = \frac{2^{\frac{R_B}{\beta}} - 1}{P_A}$, $\eta = \frac{2^{\frac{R_D}{1-\beta}} - 1}{P_{D_t}}$ and β is the spectrum partition ratio.

Proof. The proof of the Theorem 6 is similar to that of the Theorem 4. Thus, we omit the proof process here. □

B. Covet Rate Optimization

Our goal is to optimize the spectrum partition and maximum transmit power of D_r for maximizing the covert rate of cellular link from Alice to BS while guaranteeing the transmission of D2D link does not experience an outage under the overlay mode. It can be formulated as the following nonlinear optimization problem

$$\max_{\beta, P_{\max}^{D_r}} \quad R_C^o, \tag{42a}$$

$$\text{s.t.} \quad \overline{\mathbb{P}}_E^* \geq 1 - \varepsilon, \tag{42b}$$

$$0 \leq \beta \leq 1, \tag{42c}$$

$$0 \leq P_{\max}^{D_r} \leq \Omega, \tag{42d}$$

where R_C^o is the covert rate given in (39), $\overline{\mathbb{P}}_E^*$ is the average minimum detection error probability at Willie given in (23), and β is the spectrum partition factor.

To solve the optimization problem in (42), we first obtain the optimal maximum transmit power of D_r, and then obtain the optimal spectrum partition factor β. Based on these two optimal values, the MCR of the cellular link follows.

The optimal maximum transmit power of D_r is provided in the following Theorem.

Theorem 7. *We use $P_{\max}^{D_r o*}$ to denote the optimal maximum transmit power of D_r under the overlay mode.*

When $f(\varepsilon) \leq \Omega$,

$$P_{\max}^{D_r o*} = f(\varepsilon), \tag{43}$$

where $f(\varepsilon)$ is the solution of $\overline{\mathbb{P}}_E^* = 1 - \varepsilon$.

When $f(\varepsilon) > \Omega$, any $P_{\max}^{D_r o*} \in [0, \Omega]$ cannot satisfy the covertness requirement of (42b), and thus the MCR $R_C^{o*} = 0$.

Proof. The derivation process of the Theorem 7 is similar to that of the Theorem 5. Thus, we omit its derivation process here. □

We can see that the optimal maximum transmit power of D_r under the overlay mode is the same as that under the underlay mode. It is because, $P_{\max}^{D_r}$ has the same feasible solutions with the constraint of covertness requirement in (33b) and (42b) under these two modes, and the objective functions in (33a) and (42a) monotonically decrease with $P_{\max}^{D_r}$.

We now determine the optimal spectrum partition factor β^{o*}, and the MCR R_C^{o*} under the optimal $P_{\max}^{D_r o*}$ and β^{o*}. By substituting $P_{\max}^{D_r o*}$ into (42a), the objective function of (42a) can be transformed into that denoted by $R_C^o(\beta)$ only related to β. The corresponding optimization problem is given by

$$\max_{\beta} \quad R_C^o(\beta), \tag{44a}$$

$$\text{s.t.} \quad 0 \leq \beta \leq 1. \tag{44b}$$

We use β^{o*} to denote the optimal spectrum partition factor, which can be easily obtained by solving (44) using numerical search. By substituting $P_{\max}^{D_r o*}$ and β^{o*} into (42a), the MCR R_C^{o*} follows.

VI. Covert Rate under the Flexible Mode Selection

This section first provides theoretical modeling for the covert rate of cellular link from Alice to BS under the flexible mode selection, and then optimizes mode selection probability, spectrum partition factor and maximum transmit power of D_r for maximizing the covert rate.

A. Covert Rate Modeling

Based on the mode selection, the D2D pair can operate over the underlay mode with probability p and over the overlay mode with probability $1 - p$. We then formulate the covert rate denoted by R_C under the mode selection as

$$R_C = pR_C^u + (1 - p)R_C^o, \tag{45}$$

where R_C^u and R_C^o are the covert rate under the underlay mode and overlay mode given in (27) and (39), respectively.

B. Covert Rate Maximization

Our objective is to optimize the mode selection probability p, spectrum partition factor β and maximum transmit power $P_{\max}^{D_r}$ of D_r for maximizing the covert rate. We can formulate it as the following nonlinear optimization problem

$$\max_{p,\beta,P_{\max}^{D_r}} \quad R_C, \tag{46a}$$

$$\text{s.t.} \quad \overline{\mathbb{P}}_E^* \geq 1-\varepsilon, \tag{46b}$$

$$0 \leq p \leq 1, \tag{46c}$$

$$0 \leq \beta \leq 1, \tag{46d}$$

$$0 \leq P_{\max}^{D_r} \leq \Omega, \tag{46e}$$

where the covert rate R_C is given in (45), and the average minimum detection error probability $\overline{\mathbb{P}}_E^*$ is given in (23).

The following theorem gives the solution of the optimization problem in (46).

Theorem 8. *We use p^*, $P_{\max}^{D_r*}$ and β^* to denote the optimal mode selection probability, maximum transmit power of D_r and spectrum partition factor, respectively.*

When $f(\varepsilon) \leq \Omega$,

$$P_{\max}^{D_r*} = f(\varepsilon), \tag{47}$$

where $f(\varepsilon)$ is the solution of $\overline{\mathbb{P}}_E^* = 1-\varepsilon$. The two-tuple (p^*, β^*) equals to either $(0, \beta^{o*})$ or $(1, [0,1])$. The corresponding MCR R_C^* is obtained by substituting p^*, $P_{\max}^{D_r*}$ and β^* into (45).

When $f(\varepsilon) > \Omega$, any $P_{\max}^{D_r*} \in [0, \Omega]$ cannot satisfy the covertness requirement in (46b), thus $R_C^* = 0$.

Proof. To solve the optimization problem in (46), we need to decide the monotonicity property of R_C with respect to p, $P_{\max}^{D_r}$ and β. First, taking the derivation of R_C with respect to $P_{\max}^{D_r}$, we have

$$\frac{\partial R_C}{\partial P_{\max}^{D_r}} = p\frac{\partial R_C^u}{\partial P_{\max}^{D_r}} + (1-p)\frac{\partial R_C^o}{\partial P_{\max}^{D_r}}. \tag{48}$$

We know that $0 \leq p \leq 1$, $\frac{\partial R_C^u}{\partial P_{\max}^{D_r}} < 0$ and $\frac{\partial R_C^o}{\partial P_{\max}^{D_r}} < 0$. Thus, $\frac{\partial R_C}{\partial P_{\max}^{D_r}} < 0$, which indicates that R_C monotonically decreases with $P_{\max}^{D_r}$. Recall that $\overline{\mathbb{P}}_E^*$ monotonically increases with $P_{\max}^{D_r}$ proved in the derivation process of Theorem 5. We consider $f(\varepsilon)$ is the solution of $\overline{\mathbb{P}}_E^* = 1-\varepsilon$. Thus, when satisfying the constraint of (46b), $P_{\max}^{D_r} \geq f(\varepsilon)$. Note that the upper bound of $P_{\max}^{D_r}$ is Ω. If $f(\varepsilon) > \Omega$, for any $P_{\max}^{D_r*} \in [0, \Omega]$ cannot satisfy the covertness requirement in (46b) and thus $R_C^* = 0$. Otherwise, $P_{\max}^{D_r*} = f(\varepsilon)$.

By substituting $P_{\max}^{D_r*}$ into the objective function, we can obtain a function $R_C(p, \beta)$ with respect to p and β. Taking the derivation of $R_C(p, \beta)$ with respect to p, we have $\frac{\partial R_C(p,\beta)}{\partial p} = R_C^u - R_C^o$. Thus, if $R_C^u < R_C^o$, $p^* = 0$, which indicates that the D2D pair works over the overlay mode and thus $\beta^* = \beta^{o*}$. Otherwise, $p^* = 1$, which indicates that the D2D pair works over the underlay mode and thus β^* can be any value in $[0, 1]$. □

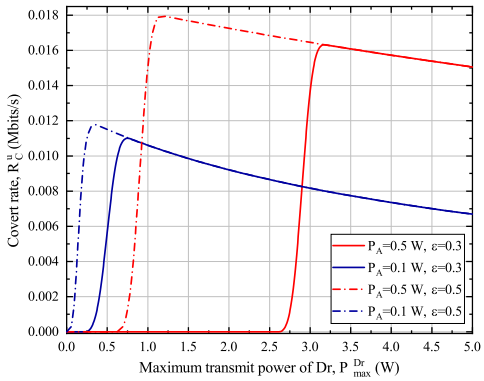

Fig. 2: The effect of $P_{\max}^{D_r}$ on R_C^u under the underlay mode.

VII. Numerical Results

In this section, extensive numerical results are presented to explore the effect of some key system parameters (e.g., p, β, Ω) on the covert rate performance under the underlay mode, the overlay mode and the mode selection. We set the following parameters as $\lambda_{i,j} = 1$, $\sigma_j^2 = 1$ W, $R_B = 0.05$ Mbits/s, $R_D = 0.05$ Mbits/s, $\phi = 0.1$, where $i \in \{A, D_t, D_r, W\}$ and $j \in \{B, W, D_r\}$, unless otherwise specified.

A. Covert Rate under the Underlay Mode

To explore the effect of the maximum transmit power $P_{\max}^{D_r}$ of D_r on the covert rate R_C^u under the underlay mode, we summarize in Fig. 2 how R_C^u varies with $P_{\max}^{D_r}$ for each setting of the following parameters $\Omega = 5$ W, $P_{D_t} = 0.1$ W, $P_{\max}^W = 1$ W, $P_A = \{0.1, 0.5\}$ W and $\varepsilon = \{0.3, 0.5\}$. We can see from Fig. 2 that as $P_{\max}^{D_r}$ increases, R_C^u first remains zero, then increases up to a maximum value, and finally decreases. This is due to the following reasons. When $P_{\max}^{D_r}$ is relatively small, the covertness requirement cannot hold, i.e., $\overline{\mathbb{P}}_E^* < 1-\varepsilon$, where $\overline{\mathbb{P}}_E^*$ is a monotonically increasing function of $P_{\max}^{D_r}$. Thus, $R_C^u = 0$. $P_{\max}^{D_r}$ continues to increase up to a threshold such that $\overline{\mathbb{P}}_E^* = 1-\varepsilon$, which corresponds to a maximum R_C^u. Recall that transmission outage probabilities P_{co}^u and P_{do}^u of Alice and D_t monotonically increase with $P_{\max}^{D_r}$, and thus R_C^u decreases as $P_{\max}^{D_r}$ increases.

Another observation of Fig. 2 indicates that for each fixed P_A, a bigger ε leads to a higher MCR. This is because a bigger ε corresponds to a smaller $1-\varepsilon$, and we know that $\overline{\mathbb{P}}_E^*$ monotonically increases as $P_{\max}^{D_r}$ increases. Thus, a smaller $P_{\max}^{D_r}$ can make that the constraint $\overline{\mathbb{P}}_E^* \geq 1-\varepsilon$ holds. Since R_C^u is a monotonically decreasing function of $P_{\max}^{D_r}$, the smaller $P_{\max}^{D_r}$ leads to a higher MCR.

To illustrate the impact of self-interference cancellation coefficient ϕ on the covert rate R_C^u, we summarize in Fig. 3 how R_C^u varies with ϕ for each setting of the following parameters $P_A = 0.1$ W, $P_{D_t} = 0.1$ W, $P_{\max}^W = 1$ W and $P_{\max}^{D_r} = \{1, 2\}$ W. We can see from Fig. 3 that R_C^u decreases with the increase of ϕ for all $P_{\max}^{D_r}$. The reason is that the increase of ϕ reduces SINR_{D_r} at the D2D receiver D_r which leads to the increase of P_{do}^u, and thus decreases R_C^u according

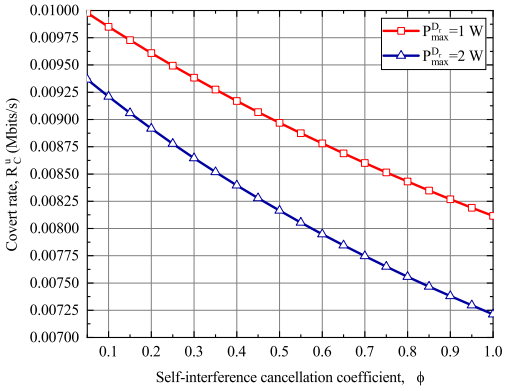

Fig. 3: The effect of ϕ on R_C^u under the underlay mode.

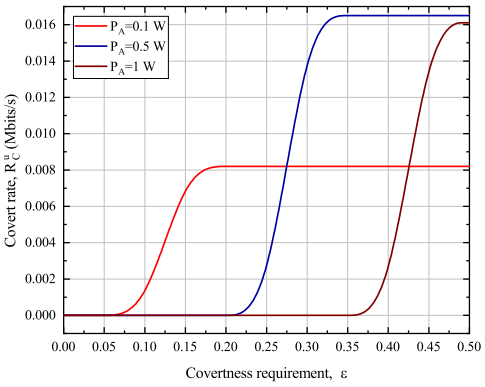

Fig. 5: The effect of ε on R_C^u under the underlay mode.

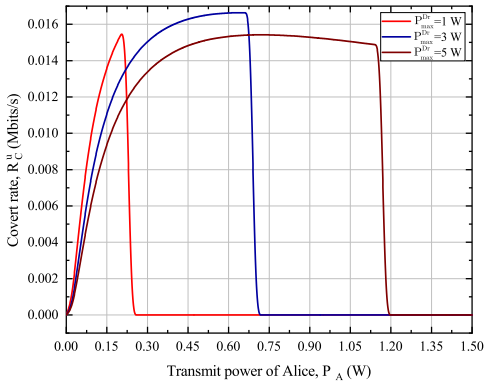

Fig. 4: The effect of P_A on R_C^u under the underlay mode.

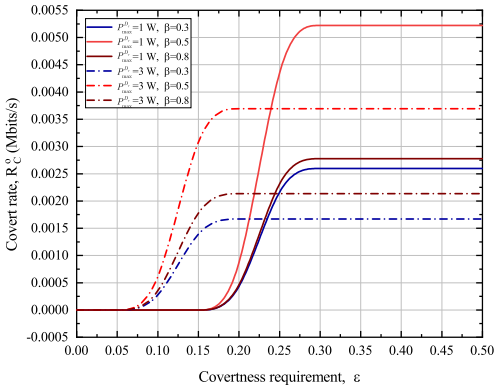

Fig. 6: The effect of ε on R_C^o under the overlay mode.

to (27). We can also observe that for a given ϕ, R_C^u decreases with the increase of $P_{\max}^{D_r}$. It can be explained as follows. When $P_{\max}^{D_r}$ increases, the interference at D_r and BS increase, which leads to the increase of P_{co}^u and P_{do}^u, and thus R_C^u decreases.

We then explore the effect of the transmit power P_A of Alice on the covert rate R_C^u under the underlay mode. We summarize in Fig. 4 how R_C^u varies with P_A for each setting of the following parameters $P_{D_t} = 0.1$ W, $P_{\max}^W = 1$ W, $\varepsilon = 0.35$ and $P_{\max}^{D_r} = \{1, 3, 5\}$ W. We can observe from Fig. 4 that when P_A increases, R_C^u first increases and then keeps zero for $P_{\max}^{D_r} = \{1, 3\}$ W, while R_C^u first increases, then decreases and finally keeps zero for $P_{\max}^{D_r} = 5$ W. This can be explained as follows. The effect of increasing P_A on R_C^u is twofold. On one hand, increasing P_A can decrease the transmission outage probability P_{co}^u of Alice, which leads to the increase of R_C^u. On the other hand, increasing P_A can also increase the transmission outage probability P_{do}^u of D_t due to negative effect of the interference, which leads to the decrease of R_C^u. As P_A is relatively small, the former dominates the latter, and thus R_C^u increases with P_A. As P_A becomes relatively large, the latter dominates the former. For the relatively small $P_{\max}^{D_r}$, the covertness requirement constraint $\overline{\mathbb{P}}_E^* \geq 1-\varepsilon$ cannot hold, and thus R_C^u reduces to zero and keeps unchanged, where $\overline{\mathbb{P}}_E^*$ is an increasing function of $P_{\max}^{D_r}$. For the relatively large $P_{\max}^{D_r}$, as P_A further increases, R_C^u first decreases and then reduces to zero when the covertness requirement constraint cannot hold.

We now proceed to investigate the effect of the covertness requirement ε on the covert rate R_C^u. Fig. 5 shows how R_C^u varies with ε for each setting of $P_{\max}^{D_r} = 3$ W, $P_{D_t} = 0.1$ W, $P_{\max}^W = 1$ W, and $P_A = \{0.1, 0.5, 1\}$ W. It can be seen from Fig. 5 that for each fixed P_A, R_C^u first keeps zero, then increases up to a constant and keeps unchanged as ε increases. This is because, when ε is relatively small, the covertness requirement constraint $\overline{\mathbb{P}}_E^* \geq 1-\varepsilon$ cannot hold, and thus $R_C^u = 0$. As ε continues to increase, the constraint holds, and thus R_C^u keeps unchanged for each fixed P_A and $P_{\max}^{D_r}$.

B. Covert Rate under the Overlay Mode

We examine the effect of covertness requirement ε on the covert rate R_C^o under the overlay mode. Fig. 6 illustrates how R_C^o varies with ε for each setting of $P_A = 0.1$ W, $P_{D_t} = 0.1$ W, $P_{\max}^W = 5$ W, $P_{\max}^{D_r} = \{1, 3\}$ W and $\beta = \{0.3, 0.5, 0.8\}$. We can see from Fig. 6 that for each fixed $P_{\max}^{D_r}$ and β, as ε increases, R_C^o first remains zero, then increases up to a constant and keeps unchanged. This is

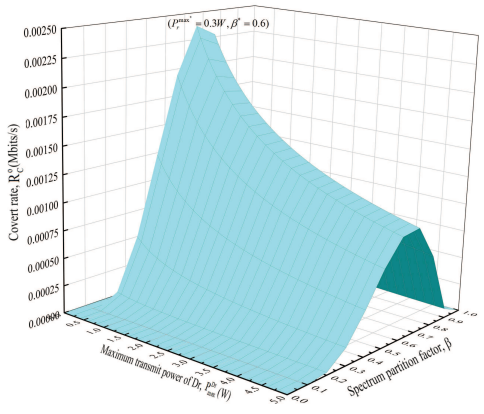

Fig. 7: The effect of $P_{\max}^{D_r}$ and β on R_C^o under the overlay mode.

due to the following reasons. A relatively small ε makes that the covertness requirement condition cannot hold, and thus $R_C^o = 0$, while as ε becomes relatively large, the condition holds, and thus R_C^o keeps an unchanged maximum value. Another careful observation of Fig. 6 shows that for each fixed $P_{\max}^{D_r}$, R_C^o given $\beta = 0.5$ is higher than that given $\beta = \{0.3, 0.8\}$, which indicates that the spectrum partition factor β needs to be carefully set for enhancing covert rate performance.

Fig. 7 illustrates the effect of $P_{\max}^{D_r}$ and β on R_C^o. As shown in Fig. 7, when β is almost zero or one, R_C^o is almost zero. Otherwise, for each fixed $P_{\max}^{D_r}$, as β increases, there exists an optimal β for maximizing R_C^o. The reasons behind this phenomenon can be explored as follows. For the former case, Alice or D_t is hardly allocated to spectrum resource such that $P_{co}^o \approx 1$ or $P_{do}^o \approx 1$, which means that $R_C^o \approx 0$. For the latter case, an increase of β can lead to an decrease of P_{co}^o and a increase of P_{do}^o, and thus there exists an optimal β for maximizing the product of $1 - P_{co}^o$ and $1 - P_{do}^o$, which leads to a maximum R_C^o. On the other hand, for a fixed β, as $P_{\max}^{D_r}$ increases, R_C^o first remains zero, then increases and finally decreases, which is similar to the phenomenon under the underlay mode. We can also see from Fig. 7 that the maximum R_C^o is achieved when $P_{\max}^{D_r o*} = 0.3$ W and $\beta^* = 0.6$.

C. Covert Rate under the Mode Selection

We study how $P_{\max}^{D_r}$, β and p affect R_C under the mode selection with the setting of $P_A = 0.5$ W, $P_{D_t} = 0.1$ W, $P_{\max}^W = 1$ W and $\varepsilon = 0.3$. Given $p = 0.5$, Fig. 8(a) illustrates the effect of $P_{\max}^{D_r}$ and β on R_C. It can be observed from Fig. 8(a) that for a fixed β, as $P_{\max}^{D_r}$ increases, R_C first keeps zero, then increases up to a maximum value and finally decreases, while as β increases, R_C keeps zero for each relatively small $P_{\max}^{D_r}$, and it first increases and decreases for each relatively large $P_{\max}^{D_r}$. The reasons behind these phenomena are similar to those under the underlay or overlay modes. We can also observe that there exist optimal $\beta^* = 0.4$ and $P_{\max}^{D_r *} = 3$ W for maximizing R_C.

Fig.8(b) illustrates the effect of p and $P_{\max}^{D_r}$ on R_C with the setting of $\beta = 0.4$. We can see from Fig. 8(b) that for each relatively large $P_{\max}^{D_r}$, an increase of p leads to an increase of R_C. This is because as p increases, the D2D pair works over the underlay mode with a higher probability p such that the transmission of D_t can confuse the detection of Willie, which leads to the increase of R_C. Another observation of Fig. 8(b) indicates that R_C achieves a maximum value when $P_{\max}^{D_r *} = 3$ W, and $p^* = 1$.

In Fig.8(c), we explore the effect of p and β on R_C with the setting of $P_{\max}^{D_r} = 3$ W. We can see from Fig.8(c) that for each fixed $p \neq 1$, as β increases, R_C first increases and then decreases. Note that when $p = 1$, R_C keeps a constant, due to the fact that the D2D pair works over the underlay mode, and thus increasing β associated with the overlay mode cannot change R_C under the underlay mode. We can also obtain a maximum R_C when $p^* = 1$ and $\beta^* \in [0, 1]$.

D. Maximum Covert Rate

We now explore the effect of upper bound Ω of maximum transmit power of D_r on the MCR under the underlay mode, overlay mode and mode selection. We summarize in Fig. 9 how the MCR varies with Ω for a setting of $P_A = 0.05$ W, $P_{D_t} = 0.1$ W, $P_{\max}^W = 1$ W and $\varepsilon = 0.3$. We can see from Fig. 9 that as Ω increases, the MCR under these three modes first keeps zero, then increases up to a maximum value and keeps unchanged. This can be explained as follows. When Ω is relatively small, $P_{\max}^{D_r} \in [0, \Omega]$ such that the covertness requirement constraint $\overline{\mathbb{P}}_E^* \geq 1 - \varepsilon$ formulated in (33b), (42b) and (46b) cannot be satisfied since $\overline{\mathbb{P}}_E^*$ is an increasing function of $P_{\max}^{D_r}$. When Ω increases up to some threshold, the constraint holds, and we know that the covert rates decrease as $P_{\max}^{D_r}$ increases under these three modes. Thus, the MCR increases up to a maximum value and keeps unchanged beyond the threshold. Specially, the concerned network under the mode selection can switch to the optimal one of the underlay and overlay modes, such that the MCR achieves the maximum one of these under the underlay and overlay modes. The results in Fig. 9 also demonstrate the correctness of Theorem 8, and provide insights that for giving a set of parameters the covert rate performance under the underlay mode is always better than that under the overlay mode, vice versa.

We proceed to examine the effect of ε on the MCR under these three modes. Fig. 10 illustrates how the MCR varies with ε for a setting of $P_A = 0.5$ W, $P_{D_t} = 0.1$ W, $P_{\max}^W = 1$ W and $\Omega = 5$ W. It can be observed from Fig. 10 that as ε increases, the MCR under three modes first keeps zero and then increases. This is due to the following reasons. When ε is relatively small, it leads to a large $1-\varepsilon$ such that the covertness requirement condition cannot hold. Thus, the MCR remains zero. When ε increases up to some threshold, the covertness requirement condition holds, i.e., $\overline{\mathbb{P}}_E^* = 1 - \varepsilon$. We know that $\overline{\mathbb{P}}_E^*$ is an increasing function of $P_{\max}^{D_r}$. Thus, as $1-\varepsilon$ decreases, $P_{\max}^{D_r}$ also decreases. Since the covert rate is a decreasing function of $P_{\max}^{D_r}$ under each mode, the MCR increases with ε. We can also observe from Fig. 10 that under the mode

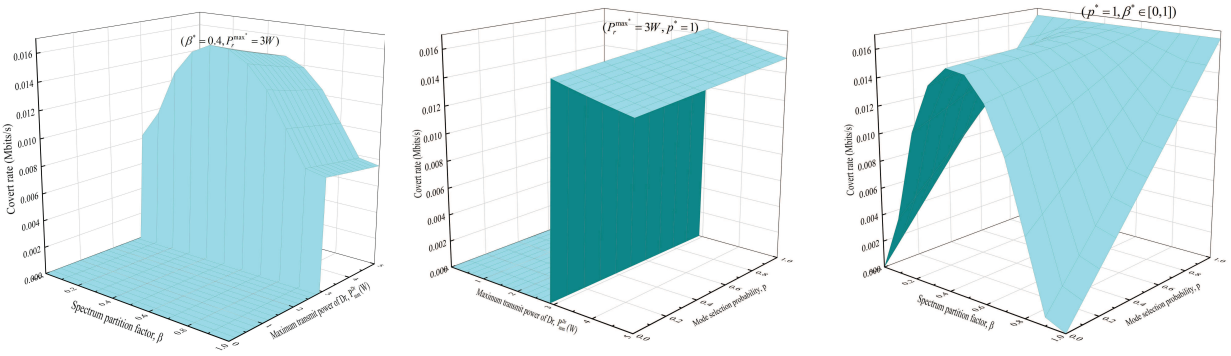

(a) R_C vs. $P_{\max}^{D_r}$ and β (b) R_C vs. p and $P_{\max}^{D_r}$ (c) R_C vs. p and β

Fig. 8: The effect of $P_{\max}^{D_r}$, β and p on R_C.

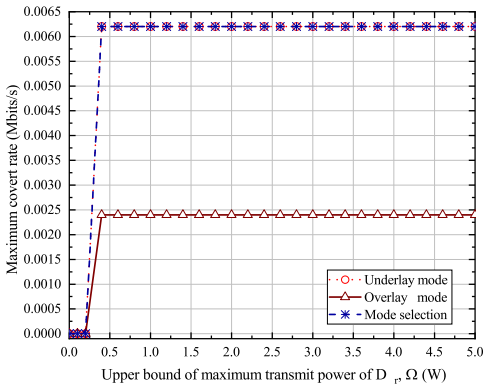

Fig. 9: The effect of Ω on the MCR.

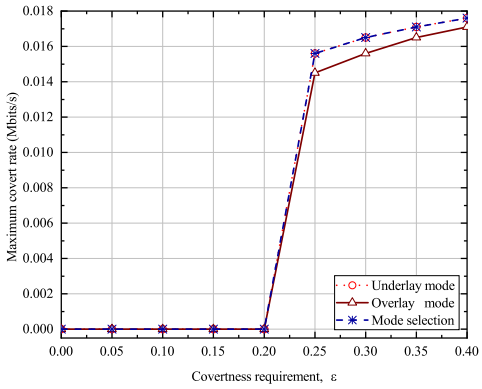

Fig. 10: The effect of ε on the MCR.

selection, as ε increases, the concerned network switches to the optimal underlay mode, where the MCR is the maximum one of these under the underlay and overlay modes.

VIII. Conclusion

This paper investigated the fundamental covert rate performance in full-duplex D2D-enabled cellular networks under the underlay mode, overlay mode and mode selection. We developed theoretical frameworks to model the covert rate and explored the corresponding covert rate maximization under these three modes, respectively. With the assistant of the full-duplex D2D receiver, both the covertness and positive covert rate can be achieved in the presence of the active warden. The results in this paper also indicate that in comparison with the underlay and overlay modes, the mode selection can lead to a significant improvement in covert rate by properly setting the mode selection probability. In particular, each mode owns its maximum achievable covert rate and corresponding optimal parameter settings (like transmit power of D_r, spectrum partition factor or mode selection probability), so a suitable mode should be selected to support various applications with different requirement on covert rate. An interesting study is to explore the covert communications of a more general scenario with multiple D2D pairs reusing the spectrum resource of a single cellular user in our future work. Another interesting study is to explore the impact of imperfect channel estimation on the covert rate maximization under the rules for power control, mode selection, and spectrum partition fraction.

References

[1] A. Asadi, Q. Wang, and V. Mancuso, "A survey on device-to-device communication in cellular networks," *IEEE Communications Surveys & Tutorials*, vol. 16, no. 4, pp. 1801–1819, 2014.

[2] M. N. Tehrani, M. Uysal, and H. Yanikomeroglu, "Device-to-device communication in 5G cellular networks: challenges, solutions, and future directions," *IEEE Communications Magazine*, vol. 52, no. 5, pp. 86–92, 2014.

[3] G. Fodor, E. Dahlman, G. Mildh, S. Parkvall, N. Reider, G. Miklós, and Z. Turányi, "Design aspects of network assisted device-to-device communications," *IEEE Communications Magazine*, vol. 50, no. 3, pp. 170–177, 2012.

[4] H. Zhu, Y. Cao, Q. Hu, W. Wang, T. Jiang, and Q. Zhang, "Multi-bitrate video caching for D2D-enabled cellular networks," *IEEE MultiMedia*, vol. 26, no. 1, pp. 10–20, 2018.

[5] B. Yang, T. Taleb, Y. Fan, and S. Shen, "Mode selection and cooperative jamming for covert communication in D2D underlaid UAV networks," *IEEE Network*, vol. 35, no. 2, pp. 104–111, 2021.

[6] S. Feng, X. Lu, S. Sun, D. Niyato, and E. Hossain, "Securing large-scale D2D networks using covert communication and friendly jamming," *IEEE Transactions on Wireless Communications*, pp. 1–1, 2023.

[7] A. Liao, Z. Gao, D. Wang, H. Wang, H. Yin, D. W. K. Ng, and M.-S. Alouini, "Terahertz ultra-massive MIMO-based aeronautical communications in space-air-ground integrated networks," *IEEE Journal on Selected Areas in Communications*, vol. 39, no. 6, pp. 1741–1767, 2021.

[8] M. Waqas, Y. Niu, Y. Li, M. Ahmed, D. Jin, S. Chen, and Z. Han, "A comprehensive survey on mobility-aware D2D communications: Principles, practice and challenges," *IEEE Communications Surveys & Tutorials*, vol. 22, no. 3, pp. 1863–1886, 2019.

[9] W. Shen, W. Hong, X. Cao, B. Yin, D. M. Shila, and Y. Cheng, "Secure key establishment for device-to-device communications," in *2014 IEEE Global Communications Conference*. IEEE, 2014, pp. 336–340.

[10] M. Haus, M. Waqas, A. Y. Ding, Y. Li, S. Tarkoma, and J. Ott, "Security and privacy in device-to-device (D2D) communication: A review," *IEEE Communications Surveys and Tutorials*, vol. 19, no. 2, pp. 1054–1079, 2017.

[11] Y. Zhang, Y. Shen, X. Jiang, and S. Kasahara, "Mode selection and spectrum partition for D2D inband communications: A physical layer security perspective," *IEEE Transactions on Communications*, vol. 67, no. 1, pp. 623–638, 2018.

[12] C. Ma, J. Liu, X. Tian, H. Yu, Y. Cui, and X. Wang, "Interference exploitation in D2D-enabled cellular networks: A secrecy perspective," *IEEE Transactions on Communications*, vol. 63, no. 1, pp. 229–242, 2015.

[13] Y. J. Tolossa, S. Vuppala, G. Kaddoum, and G. Abreu, "On the uplink secrecy capacity analysis in D2D-enabled cellular network," *IEEE Systems Journal*, pp. 2297–2307, 2017.

[14] W. Wang, K. C. Teh, and K. H. Li, "Enhanced physical layer security in D2D spectrum sharing networks," *IEEE Wireless Communications Letters*, vol. 6, no. 1, pp. 106–109, 2016.

[15] R. Khan, P. Kumar, D. N. K. Jayakody, and M. Liyanage, "A survey on security and privacy of 5G technologies: Potential solutions, recent advancements, and future directions," *IEEE Communications Surveys & Tutorials*, vol. 22, no. 1, pp. 196–248, 2019.

[16] S. Fang, Y. Liu, and P. Ning, "Wireless communications under broadband reactive jamming attacks," *IEEE Transactions on Dependable and Secure Computing*, vol. 13, no. 3, pp. 394–408, 2015.

[17] S. Yan, X. Zhou, J. Hu, and S. V. Hanly, "Low probability of detection communication: Opportunities and challenges," *IEEE Wireless Communications*, vol. 26, no. 5, pp. 19–25, 2019.

[18] B. A. Bash, D. Goeckel, and D. Towsley, "Limits of reliable communication with low probability of detection on AWGN channels," *IEEE Journal on Selected Areas in Communications*, vol. 31, no. 9, pp. 1921–1930, 2013.

[19] C. Gao, B. Yang, X. Jiang, H. Inamura, and M. Fukushi, "Covert communication in relay-assisted IoT systems," *IEEE Internet of Things Journal*, vol. 8, no. 8, pp. 6313–6323, 2021.

[20] R. Sun, B. Yang, S. Ma, Y. Shen, and X. Jiang, "Covert rate maximization in wireless full-duplex relaying systems with power control," *IEEE Transactions on Communications*, vol. 69, no. 9, pp. 6198–6212, 2021.

[21] M. Ahmadipour, S. Salehkalaibar, M. H. Yassaee, and V. Y. Tan, "Covert communication over a compound discrete memoryless channel," in *2019 IEEE International Symposium on Information Theory (ISIT)*. IEEE, 2019, pp. 982–986.

[22] L. Wang, G. W. Wornell, and L. Zheng, "Limits of low-probability-of-detection communication over a discrete memoryless channel," pp. 2525–2529, 2015.

[23] K. Li, P. A. Kelly, and D. Goeckel, "Optimal power adaptation in covert communication with an uninformed jammer," *IEEE Transactions on Wireless Communications*, vol. 19, no. 5, pp. 3463–3473, 2020.

[24] C. Wang, Z. Li, J. Shi, and D. W. K. Ng, "Intelligent reflecting surface-assisted multi-antenna covert communications: Joint active and passive beamforming optimization," *IEEE Transactions on Communications*, 2021.

[25] K. Shahzad, X. Zhou, S. Yan, J. Hu, F. Shu, and J. Li, "Achieving covert wireless communications using a full-duplex receiver," *IEEE Transactions on Wireless Communications*, vol. 17, no. 12, pp. 8517–8530, 2018.

[26] X. Chen, W. Sun, C. Xing, N. Zhao, Y. Chen, F. R. Yu, and A. Nallanathan, "Multi-antenna covert communication via full-duplex jamming against a warden with uncertain locations," *IEEE Transactions on Wireless Communications*, vol. 20, no. 8, pp. 5467–5480, 2021.

[27] M. Zheng, A. Hamilton, and C. Ling, "Covert communications with a full-duplex receiver in non-coherent rayleigh fading," *IEEE Transactions on Communications*, vol. 69, no. 3, pp. 1882–1895, 2020.

[28] C. Wang, Z. Li, and D. W. K. Ng, "Covert rate optimization of millimeter wave full-duplex communications," *IEEE Transactions on Wireless Communications*, vol. 21, no. 5, pp. 2844–2861, 2021.

[29] Y. Jiang, L. Wang, H. Zhao, and H. H. Chen, "Covert communications in D2D underlaying cellular networks with power domain NOMA," *IEEE Systems Journal*, vol. PP, no. 99, pp. 1–12, 2020.

[30] X. Shi, D. Wu, C. Yue, C. Wan, and X. Guan, "Resource allocation for covert communication in D2D content sharing: A matching game approach," *IEEE Access*, vol. 7, pp. 72 835–72 849, 2019.

[31] X. Shi, D. Wu, C. Wan, M. Wang, and Y. Zhang, "Trust evaluation and covert communication-based secure content delivery for D2D networks: A hierarchical matching approach," *IEEE Access*, vol. 7, pp. 134 838–134 853, 2019.

[32] Y. Jiang, L. Wang, and H.-H. Chen, "Covert communications in D2D underlaying cellular networks with antenna array assisted artificial noise transmission," *IEEE Transactions on Vehicular Technology*, vol. 69, no. 3, pp. 2980–2992, 2020.

[33] Y. Yang, B. Yang, S. Shen, Y. She, and T. Taleb, "Covert rate study for full-duplex D2D communications underlaid cellular networks," *IEEE Internet of Things Journal*, vol. 10, no. 17, pp. 15 223–15 237, 2023.

[34] H. Rao, M. Wu, J. Wang, W. Tang, S. Xiao, and S. Li, "D2D covert communications with safety area," *IEEE Systems Journal*, 2020.

[35] L. Sun, T. Xu, S. Yan, J. Hu, X. Yu, and F. Shu, "On resource allocation in covert wireless communication with channel estimation," *IEEE Transactions on Communications*, vol. 68, no. 10, pp. 6456–6469, 2020.

[36] J. Hu, K. Shahzad, S. Yan, X. Zhou, F. Shu, and J. Li, "Covert communications with a full-duplex receiver over wireless fading channels," in *2018 IEEE International Conference on Communications (ICC)*, 2018, pp. 1–6.

[37] L. Yang, W. Yang, S. Xu, L. Tang, and Z. He, "Achieving covert wireless communications using a full-duplex multi-antenna receiver," in *2019 IEEE 5th International Conference on Computer and Communications (ICCC)*, 2019, pp. 912–916.

[38] S. Yan, Y. Cong, S. V. Hanly, and X. Zhou, "Gaussian signalling for covert communications," *IEEE Transactions on Wireless Communications*, vol. 18, no. 7, pp. 3542–3553, 2019.

[39] Z. Zhang, X. Chai, K. Long, A. V. Vasilakos, and L. Hanzo, "Full duplex techniques for 5G networks: self-interference cancellation, protocol design, and relay selection," *IEEE Communications Magazine*, vol. 53, no. 5, pp. 128–137, 2015.

[40] T. V. Sobers, B. A. Bash, S. Guha, D. Towsley, and D. Goeckel, "Covert communication in the presence of an uninformed jammer," *IEEE Transactions on Wireless Communications*, vol. 16, no. 9, pp. 6193–6206, 2017.

Ranran Sun received the B.S. and M.S. degrees in computer science from the Henan University of Science and Technology, Luoyang, China, in 2014 and 2017, respectively, and the Ph.D. degree with the School of Computer Science and Technology, Xidian University, Xi'an, China. She is currently a Postdoctoral Researcher with the Hangzhou Institute of Technology, Xidian University, Hangzhou, China. Her research interest focuses on the covert communication in physical layer.

Huihui Wu (Member, IEEE) received the B.S. degree from the Department of Computer Science and Technology, Sichuan University, Chengdu, China, in 2016, the M.S. degree from the Department of Computer Science and Technology, Xidian University, Xi'an, China, in 2019, and the Ph.D. degree from the School of Systems Information Science, Future University Hakodate, Hakodate, Japan, in 2021. She is currently a Postdoctoral Researcher with the Department of Automation, Tsinghua University, China. Her research interests include physical-layer security, covert wireless communication, and integrated sensing and communication.

Bin Yang received his Ph.D. degree in systems information science from Future University Hakodate, Japan in 2015. He was a research fellow with the School of Electrical Engineering, Aalto University, Finland, from Jul. 2020 to Nov. 2021. He is currently a professor with the School of Computer and Information Engineering, Chuzhou University, China. His research interests include unmanned aerial vehicle networks, cyber security and Internet of Things.

Yulong Shen (Member, IEEE) received the B.S. and M.S. degrees in computer science and the Ph.D. degree in cryptography from Xidian University, Xi'an, China, in 2002, 2005, and 2008, respectively. He is currently a Professor with the School of Computer Science and Technology, Xidian University, where he is also an Associate Director of the Shaanxi Key Laboratory of Network and System Security and a member of the State Key Laboratory of Integrated Services Networks. His research interests include wireless network security and cloud computing security. He has also served on the technical program committees of several international conferences, including ICEBE, INCoS, CIS, and SOWN.

Weidong Yang received his B.S. in industrial automation, and M.S. and Ph.D. degree in Computer Science from Xidian University in China in 1999, 2005, and 2008, respectively. He is now a professor in Hangzhou Institute of Technology, Xidian University. He is also a senior member of China Computer Federation (CCF). His research focuses on wireless networks security, privacy protection, and vehicular ad hoc networks, and so on.

Xiaohong Jiang (Senior Member, IEEE) received his B.S., M.S. and Ph.D degrees in 1989, 1992, and 1999 respectively, all from Xidian University, China. He is currently a full professor of Future University Hakodate, Japan. Before joining Future University, Dr. Jiang was an Associate professor, Tohoku University, from Feb. 2005 to Mar. 2010. Dr. Jiang's research interests include computer communications networks, mainly wireless networks and optical networks, network security, routers/switches design, etc. He has published over 300 technical papers at premium international journals and conferences, which include over 70 papers published in top IEEE journals and top IEEE conferences, like IEEE/ACM Transactions on Networking, IEEE Journal of Selected Areas on Communications, IEEE Transactions on Parallel and Distributed Systems, IEEE INFOCOM.

Tarik Taleb (Senior Member, IEEE) received the B.E. degree Information Engineering with distinction and the M.Sc. and Ph.D. degrees in Information Sciences from Tohoku University, Sendai, Japan, in 2001, 2003, and 2005, respectively. He is currently a Full Professor with the Faculty of Electrical Engineering and Information Technology, Ruhr University Bochum. He is the founder and director of the MOSA!C Lab (www.mosaic-lab.org). Between Oct. 2014 and Dec. 2021, he was a Professor at the School of Electrical Engineering, Aalto University, Finland. Prior to that, he was working as Senior Researcher and 3GPP Standards Expert at NEC Europe Ltd, Heidelberg, Germany. Before joining NEC and till Mar. 2009, he worked as assistant professor at the Graduate School of Information Sciences, Tohoku University, Japan, in a lab fully funded by KDDI, the second largest mobile operator in Japan. From Oct. 2005 till Mar. 2006, he worked as research fellow at the Intelligent Cosmos Research Institute, Sendai, Japan. His research interests lie in the field of telco cloud, network softwarization & network slicing, AI-based software defined security, immersive communications, mobile multimedia streaming, and next generation mobile networking. He has been also directly engaged in the development and standardization of the Evolved Packet System as a member of 3GPP's System Architecture working group 2. He served as the general chair of the 2019 edition of the IEEE Wireless Communications and Networking Conference (WCNC'19) held in Marrakech, Morocco. He was the guest editor in chief of the IEEE JSAC Series on Network Softwarization & Enablers. He was on the editorial board of the IEEE Transactions on Wireless Communications, IEEE Wireless Communications Magazine, IEEE Journal on Internet of Things, IEEE Transactions on Vehicular Technology, IEEE Communications Surveys & Tutorials, and a number of Wiley journals. Till Dec. 2016, he served as chair of the Wireless Communications Technical Committee.